RISC

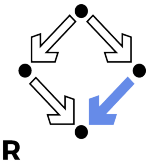

RESEARCH INSTITUTE FOR SYMBOLIC COMPUTATION

JKU

JOHANNES KEPLER UNIVERSITY LINZ

Analytic results on the massive three-loop form factors: gluonic contributions

J. Bluemlein, A. De Freitas, P. Marquard, J. Obrovsky, C. Schneider

September 2026

RISC Report Series No. 26-12

ISSN: 2791-4267 (online)

Available at https://doi.org/10.35011/risc.26-12

This work is licensed under a CC BY 4.0 license.

Editors: RISC Faculty
B. Buchberger, R. Hemmecke, T. Kutsia, G. Landsmann, P. Paule, V. Pillwein, N. Popov, S. Radu, G. Regensburger, J. Schicho, C. Schneider, W. Schreiner, W. Windsteiger, F. Winkler.

JOHANNES KEPLER UNIVERSITY LINZ
Altenberger Str. 69
4040 Linz, Austria
www.jku.at
DVR 0093696

DESY 26–118
RISC Report number 26–12
September 2026

arXiv:2609.22034 [hep-ph]

Analytic results on the massive three-loop form factors: gluonic contributions

J. Blümlein[a,b], A. De Freitas[c], P. Marquard[a], J. Obrovsky[c], and C. Schneider[c]

[a] *Deutsches Elektronen–Synchrotron DESY, Platanenallee 6, 15738 Zeuthen, Germany*

[b] *Institut für Theoretische Physik III, IV, TU Dortmund, Otto-Hahn Straße 4, 44227 Dortmund, Germany*

[c] *Johannes Kepler University Linz, Research Institute for Symbolic Computation (RISC), Altenbergerstraße 69, A–4040, Linz, Austria*

Abstract

We compute the gluonic contributions to the three-loop heavy-quark form factors for the vector, axial-vector, scalar, and pseudoscalar currents. In the low-energy limit, $q^2/m^2 \to 0$, we used guessing algorithms to derive closed-form difference and differential equations from the rational sequences associated with the multiple zeta values and other constants appearing in the expansion coefficients, which required up to 26000 coefficients in the most demanding cases. Part of the results are obtained analytically in terms of harmonic polylogarithms and square-root valued iterated integrals by solving the obtained differential equations. For the remaining contributions, arbitrarily deep series expansions around the singularities of the form factors can be obtained by matching local expansions at intermediate points and by exploiting the differential equations obeyed by the functions associated with each transcendental constant in the expansions around $s = q^2/m^2 = 0$. For all these calculations advanced computer algebra methods have been employed. By using analytic continuation methods for differential equations matching the expansions at different values of s and using PSLQ, we derive analytic results in the high-energy limit, $q^2/m^2 \to \infty$. The expansion coefficients are expressed in terms of multiple zeta values up to weight $\mathsf{w} = 6$ together with three additional constants, two related to sixth-root-of-unity letters and one associated with quadratic-form implied iterated integrals. We also derive deep expansions about the threshold and pseudo-threshold. Numerical results are presented in the whole kinematic range and compared to results in the literature.

1 Introduction

The massive form factors associated with the vector, axial-vector, scalar, and pseudoscalar currents describe the coupling of virtual bosons to a pair of massive quarks in Quantum Chromodynamics (QCD) and Quantum Electrodynamics (QED). They constitute fundamental building blocks for precision calculations involving heavy quarks and enter a wide range of observables relevant to collider phenomenology, including heavy-quark production and Higgs boson decays. The high experimental precision achieved in measurements of these processes requires equally precise theoretical predictions, motivating the computation of the corresponding form factors at increasingly high loop orders.

Beyond their phenomenological relevance, massive form factors provide one of the simplest settings for investigating the infrared structure of gauge theories with massive particles. They therefore play a central role in the study of infrared singularities and serve as benchmark quantities for the development of modern methods for multi-loop calculations.

The evaluation of the three-loop massive form factors represents a particularly challenging problem due to the large number of contributing Feynman diagrams and the complexity of the associated Feynman integrals, which involve structures beyond standard harmonic polylogarithms and related functions.[1] Considerable progress has been achieved in recent years. Partial analytic results for the three-loop form factors have been obtained in Refs. [2–13], while complete numerical results at this order were presented in Refs. [14–19].[2]

In this paper we complete the analytic determination of the three-loop QCD form factors by computing the purely gluonic contributions, thereby complementing our previous calculation of the quarkonic contributions presented in Ref. [13].[3] While the planar color contributions were obtained previously in Ref. [8], the present work provides the first complete analytic treatment including all non-planar diagrams. The vector, axial-vector, scalar and pseudoscalar form factors are given by

$$F_I(s) = 1 + \sum_{k=1}^{\infty} a_s^k(m^2) F_I^{(k)}(s), \tag{1.1}$$

where

$$s =: \frac{q^2}{m^2}, \tag{1.2}$$

and q^2 denotes the virtuality of the incoming current, m the heavy-quark mass, and $a_s = \alpha_s/(4\pi)$ is the running coupling constant renormalized in the $\overline{\rm MS}$ scheme, cf. Refs. [20–28]. For the analytic representation of the form factors, it is convenient to introduce the variable x, related to the dimensionless kinematic variable s by

$$s = -\frac{(1-x)^2}{x} \qquad \text{and} \qquad x = \frac{\sqrt{4-s}-\sqrt{-s}}{\sqrt{4-s}+\sqrt{-s}}. \tag{1.3}$$

Our approach relies as far as possible on analytic and symbolic methods. As in many multi-loop calculations, the amplitudes are first reduced to a set of master integrals, which satisfy coupled systems of differential equations. The main methodological advance of this work is the systematic exploitation of these equations to generate high-order expansions in the low energy limit. The resulting expansion coefficients are then used to derive recursion relations and differential

[1] For a survey see Ref. [1].

[2] Complete analytic results are known at $s = 0$ in the form of series expansions.

[3] For QED the QCD color factors are replaced according to $C_F = (N_c^2-1)/(2N_c) \to 1$, $T_F = 1/2 \to 1$, and $C_A = N_c \to 0$, with $N_c = 3$ in QCD.

equations from the sequences of rational numbers associated with the transcendental constants appearing in the expansions. This is done first at the level of the master integrals, and later at the level of the full physical expressions for the form factors. The most challenging differential equations do not factorize into first-order operators. In these cases we employ Frobenius' method [29], constructing high-order local series expansions [30–34] around regular and singular points and matching overlapping expansions to obtain analytic continuations throughout the entire kinematic range.

The form factors have a threshold at $s = 4$ and a pseudo-threshold at $s = 16$. A main result of the present paper is the analytic result for the massive three-loop form factors in the high energy limit $x \to 0$ or $s \to \infty$, computed for the first time. At other characteristic points, we provide deep series expansions. Furthermore, we provide semi-analytic series representations at a relative accuracy of $O(10^{-30})$ in `Mathematica` format and associated numerical implementations in the whole kinematic domain.

The paper is organized as follows. In Section 2, we describe the structure of vector, axial-vector, scalar, and pseudoscalar currents in terms of form factors and outline the basic calculation strategies. While these strategies have already been employed by us to calculate the quarkonic parts of the three-loop form factors in Refs. [12, 13], the more challenging gluonic case required substantial refinements. These improvements are carried out in the three following sections. Section 3 derives the coefficients for the series expansions of the form factors at $s = 0$ ($x = 1$). Section 4 presents the guessing of their underlying recurrences and differential equations, and Section 5 derives expansions at other relevant expansion points using efficient methods of analytic continuation. Based on these refinements, in Section 6 we describe how the analytic high energy result in the limit $s \to \infty$ is obtained. Series expansions around $s = 4$ and $s = 16$ are discussed in Section 7 and the conclusions are given in Section 8. The ancillary files to the present paper contain computer-readable analytic codes. They are described in Appendix A.

2 The basic calculation strategy

The gluonic contributions to the form factors arise exclusively from diagrams in which only gluons are exchanged between the external heavy quarks. This is in contrast to the considerably simpler quarkonic contributions studied in Refs. [12, 13], which originate from diagrams containing internal massless and massive quark loops. Representative three-loop gluonic diagrams are shown in Figure 1. The Feynman diagrams are generated by `QGRAF` [35], the Lorentz- and Dirac-algebra is carried out in $D = 4 - 2\varepsilon$ dimensions using `Form` [36, 37] and the color algebra is performed by `Color` [38].

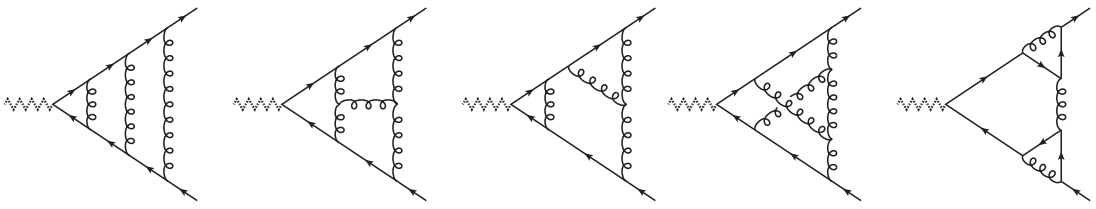

Figure 1: Sample of diagrams required for the calculation of three-loop massive form factors. The solid arrow lines represent massive quarks, while the dotted zigzag line represents any of the possible currents, and the curly lines gluons.

For the description of the different form factors we use the following conventions, see also Ref. [13]. Depending on the nature of the boson coupling to the heavy-quark pair, there are four types of three-point amplitudes. For a spin-1 vector boson, the vertex function is

$$\Gamma^{\mu}_{V,cd} = -iv_Q\delta_{cd}\left(\gamma^{\mu}\ F_{V,1}(s) + \frac{i}{2m}\sigma^{\mu\nu}q_{\nu}\ F_{V,2}(s)\right), \tag{2.1}$$

where $\sigma^{\mu\nu} = \frac{i}{2}[\gamma^{\mu},\gamma^{\nu}]$, c and d are the quark color indices, and v_Q is the corresponding Standard Model vector coupling. The axial-vector vertex is given by

$$\Gamma^{\mu}_{A,cd} = -ia_Q\delta_{cd}\left(\gamma^{\mu}\gamma_5\ F_{A,1}(s) + \frac{1}{2m}q^{\mu}\gamma_5\ F_{A,2}(s)\right), \tag{2.2}$$

where a_Q denotes the Standard Model axial-vector coupling. For a spin-0 scalar boson,

$$\Gamma_{S,cd} = -\frac{m}{v}s_Q\delta_{cd}F_S(s), \tag{2.3}$$

v is the Higgs vacuum expectation value and s_Q is the scalar coupling. Finally, the pseudoscalar vertex is given by

$$\Gamma_{P,cd} = -i\frac{m}{v}p_Q\delta_{cd}\gamma_5F_P(s), \tag{2.4}$$

and p_Q is the pseudoscalar coupling.

The vector and axial-vector form factors are extracted by applying the projectors

$$P_{V,i} = \frac{i}{v_Q}\frac{\delta_{cd}}{N_c}\frac{\not{q}_2 - m}{m}\left(\gamma_{\mu}g^{(1)}_{V,i} + \frac{1}{2m}(q_{2\mu} - q_{1\mu})g^{(2)}_{V,i}\right)\frac{\not{q}_1 + m}{m}, \tag{2.5}$$

$$P_{A,i} = \frac{i}{a_Q}\frac{\delta_{cd}}{N_c}\frac{\not{q}_2 - m}{m}\left(\gamma_{\mu}\gamma_5g^{(1)}_{A,i} + \frac{1}{2m}(q_{1\mu} + q_{2\mu})\gamma_5g^{(2)}_{A,i}\right)\frac{\not{q}_1 + m}{m}, \tag{2.6}$$

followed by traces over the spinor and color indices. Here q_1 and q_2 denote the heavy-quark momenta, satisfying $q = q_1 + q_2$. The coefficients $g^{(k)}_{I,i}$ are given by

$$g^{(1)}_{V,1} = \frac{1}{4(1-\varepsilon)(4-s)}, \qquad g^{(2)}_{V,1} = \frac{3-2\varepsilon}{(1-\varepsilon)(s-4)^2}, \tag{2.7}$$

$$g^{(1)}_{V,2} = -\frac{1}{(1-\varepsilon)(4-s)s}, \qquad g^{(2)}_{V,2} = -\frac{2((1-\varepsilon)s+2)}{(1-\varepsilon)(4-s)^2s}, \tag{2.8}$$

$$g^{(1)}_{A,1} = \frac{1}{4(1-\varepsilon)(4-s)}, \qquad g^{(2)}_{A,1} = -\frac{1}{(1-\varepsilon)(4-s)s}, \tag{2.9}$$

$$g^{(1)}_{A,2} = -\frac{1}{(1-\varepsilon)(4-s)s}, \qquad g^{(2)}_{A,2} = \frac{2(\varepsilon(s-4)-s+6)}{(1-\varepsilon)(4-s)s^2}. \tag{2.10}$$

For later convenience, we also introduce the individual contributions multiplying the functions $g^{(k)}_{I,i}$ after projection. That is, we decompose the projected form factors as

$$F_{V,i}(s) = g^{(1)}_{V,i}F_{v,1}(s) + g^{(2)}_{V,i}F_{v,2}(s), \qquad i = 1,2, \tag{2.11}$$

$$F_{A,i}(s) = g^{(1)}_{A,i}F_{a,1}(s) + g^{(2)}_{A,i}F_{a,2}(s), \qquad i = 1,2. \tag{2.12}$$

The scalar and pseudoscalar form factors are obtained analogously by applying the projectors

$$P_S = -\frac{v}{2ms_Q}\frac{\delta_{cd}}{N_c(4-s)}\frac{\not{q}_2 - m}{m}\frac{\not{q}_1 + m}{m}, \tag{2.13}$$

$$P_P = -\frac{v}{2mp_Q}\frac{\delta_{cd}}{N_c s}\frac{\not{q}_2 - m}{m} i\gamma_5 \frac{\not{q}_1 + m}{m}\,, \tag{2.14}$$

and taking the corresponding spinor and color traces.

In a similar way as in Eqs. (2.11–2.12), we extract the s-dependent part of the projectors by defining $F_s(s)$ and $F_p(s)$ as follows

$$F_S(s) = \frac{1}{2(s-4)} F_s(s)\,, \tag{2.15}$$

$$F_P(s) = -\frac{1}{2s} F_p(s)\,. \tag{2.16}$$

In the following we only consider the three-loop contributions. In QCD, these form factors are decomposed in terms of the $\mathrm{SU}(N_c)$ color factors as follows

$$F_I(s) = \sum_{j=1}^{3} C_j F_{I;j}(s), \tag{2.17}$$

where the color factors C_j are given by

$$C_1 = C_F^3\,, \quad C_2 = C_A C_F^2\,, \quad C_3 = C_A^2 C_F. \tag{2.18}$$

To simplify the notation, we henceforth use a single composite index I. Depending on the context, I denotes either one of the scalar and pseudoscalar form factors, $I \in \{S, P\}$, or one of the vector and axial-vector form factors, $I \in \{(V,1),(V,2),(A,1),(A,2)\}$. Likewise, when referring to the projected components appearing in Eqs. (2.11–2.12) and Eqs. (2.15–2.16), we use $I \in \{(v,1)\,,\,(v,2)\,,\,(a,1)\,,\,(a,2)\,,\,s\,,\,p\}$.

The renormalization of the form factors has been described in detail in Ref. [13] before. The mass and the wave function of the heavy quark have been renormalized using the on-shell scheme. For the Yukawa coupling in the scalar and pseudoscalar form factors, we also used the $\overline{\rm MS}$ renormalization scheme. All the necessary renormalization constants are available, including the description of the infrared singularities, see Refs. [39–53].

The Feynman amplitudes are reduced to master integrals (MIs) by applying integration-by-parts (IBP) reduction [54–59], using the package `Crusher` [60]. The master integrals admit Laurent expansions in ε containing pole terms. One forms differential equations for the master integrals. By a formal Taylor expansions around $y = 1 - x$

$$F(x) = \sum_{n=0}^{\infty} a(n) y^n \tag{2.19}$$

one obtains expansion coefficients $a(n)$, which serve as input sets for the method of arbitrary high moments, cf. Ref. [61]. Using these sets of coefficients for the MIs one obtains the corresponding series expansion for the amplitudes, labeled by the color factors, zeta values [62], and powers in the dimensional parameter ε from $O(1/\varepsilon^3)$ to $O(\varepsilon^0)$. Throughout the paper, the following constants appear[4]

$$l_2 = \ln(2)\,, \quad \zeta_k = \zeta(k) = \sum_{l=1}^{\infty} \frac{1}{l^k},\ k \geq 2\,, \quad a_n = \mathrm{Li}_n\left(\frac{1}{2}\right),\ n \geq 4\,, \tag{2.20}$$

[4]In the master integrals multiple zeta values [62] up to $\mathsf{w} = 9$ and ζ_{11} contribute, cf. [12], most of which cancel in the amplitude.

where $\zeta(k)$ is the Riemann ζ function evaluated at integer values $k \geq 2$, and

$$\mathrm{Li}_n(x) = \sum_{k=1}^{\infty} \frac{x^k}{k^n}, \quad |x| \leq 1, \tag{2.21}$$

are the classical polylogarithms, [63–65].

In the following we describe the basic tactic we used to compute these form factors. Their amplitudes are given by 417 MIs,

$$F_{I;j}(s) = c_1(\varepsilon, s)M_1(\varepsilon, s) + \cdots + c_{417}(\varepsilon, s)M_{417}(\varepsilon, s) \tag{2.22}$$

with rational functions $c_i(\varepsilon, s)$ in s and ε. A crucial property is that the form factors and the underlying master integrals can be given as a Laurent series expansion in ε, starting from $O(\varepsilon^{-3})$, and as power series in s. Since the coefficients $c_i(\varepsilon, s)$ also contain coefficients with factors $1/\varepsilon^k$ with $-3 \leq k \leq 10$, one needs the ε-expansion of the the MIs up to ε^k to determine the first four coefficients of the ε-expansion of the form factors. Besides the representation (2.22), the IBP reduction techniques delivers a coupled system of first-order linear differential equations in terms of the master integrals. In particular, given a finite number of initial values (the first coefficients of the expansions in s and ε), one can determine all the coefficients in s up to a certain order in ε. Given this available representation (2.22) together with the coupled system, the overall strategy of this article is based on the large moment method [61], which can be summarized as follows.

I Compute sufficiently many coefficients in s, say ρ, up to a certain order in ε of the series representations of the master integrals by using the coupled system together with the available initial values; see Section 3.

II Plug in the truncated power series solutions of the MIs into (2.22) and expand the expressions to derive ρ coefficients in s up to a certain order in ε of the series representation of the F_I's. Note that the coefficients are given as a linear combination of the constants

$$\begin{aligned} &\kappa_1 = 1, \quad \kappa_2 = \zeta_2, \quad \kappa_3 = \zeta_3, \quad \kappa_4 = l_2\zeta_2, \quad \kappa_5 = \zeta_2^2, \\ &\kappa_6 = a_4, \quad \kappa_7 = l_2^4, \quad \kappa_8 = l_2^2\zeta_2, \quad \kappa_9 = \zeta_2\zeta_3, \quad \kappa_{10} = \zeta_5, \end{aligned} \tag{2.23}$$

which come from the initial values of the MIs and the color factors given in (2.18). More precisely, one obtains a finite list of rational numbers for each form factor and each $C_i\kappa_j\varepsilon^k$ with $1 \leq i \leq 3$, $1 \leq j \leq 10$ and $-3 \leq k \leq 0$; see Section 3 for calculation details and Section 4 for examples.

III For each finite list of rational numbers $(H(n))_{n=0}^{\rho-1}$ guess a linear recurrence and a linear differential equation, cf. Refs. [66–68] of the power series $h(s) = \sum_{n=0}^{\infty} H(n)s^n$; see Section 4.

IV Using this information utilize the recurrence solver of `Sigma` [69–71] in the setting of difference rings [72–86] to determine for which physical components the coefficients are expressible in terms of iterative sums. Then transform the underlying functions of their power series representation in terms of iterative integrals using the package `HarmonicSums` [87, 88]. Furthermore, techniques are necessary to handle finite binomial sums, cf. Refs. [89, 90], cf. Section 4. All those closed form representations can be straightforwardly evaluated at any expansion point using techniques described in Refs. [91–94].

V For all contributions where the recurrences and differential equations are not first-order factorizable (i.e., the full solution space cannot be given in terms of iterative sums/integrals), perform analytic continuations and assemble the final result to derive representations of all the form factors at other expansion points; see Section 5.

We note that the required number ρ of coefficients is determined by the guessing method. If one fails to guess a recurrence or differential equation from the given number of coefficients in Step III, one has to produce more coefficients in Steps I and II until one succeeds.

Several ingredients of the calculation were already employed in the quarkonic computation of Ref. [13]. The gluonic case is, however, considerably more involved. Because of this, a number of new techniques had to be developed in order to complete the calculation.

3 Computing coefficients from the coupled systems

For the gluonic case of the form factor, we obtain a coupled system of 419 MIs that can be hierarchically structured into 147 recursively defined sub-systems obtained by the integration-by parts reduction [54–60]. The smallest sub-systems have dimension 1 and the largest ones have dimension 10. In this way, we can apply the large moment method in a bottom-up fashion for these reasonable sized 147 sub-systems. In addition, the physical expressions (scalar, pseudoscalar, vector, axial-vector) in the different color factors are given by a linear combination of these MIs, as shown in Eq. (2.17). After compactification of terms [95], the input obtained amounts to about 5 GB.

In the following we focus on such a given coupled system of first-order linear differential equations in terms of the unknown MIs $M_1(s), \ldots, M_\lambda(s)$ with $1 \leq \lambda \leq 10$ that have a power series representation $M_i(s) = \sum_{n=0}^{\infty} G_i(n) s^n$. Then the large moment method introduced in [61] deals with the problem to compute efficiently the coefficients $G_i(n)$ with $0 \leq n < \rho$ for some large ρ; in simpler cases ρ may range between 500 and 10000. We note that the inhomogeneous part depends on the master integrals coming from the sub-sectors below. Here we assume that we have computed already the first ρ coefficients of their power series expansions, either by other simpler methods or our large moment method applied recursively. The underlying steps can be summarized as follows.

I.1 We uncouple the given system. Among the available algorithms, we mainly use Gauß' and Zürcher's algorithm implemented in the `OreSys` package [96]. For further details we refer to Refs. [97, 98].

I.2 Based on the different uncoupling algorithms, we obtain one (or several) scalar differential equations

$$b_0(s)M(s) + b_1(s)\frac{d}{ds}M(s) + \cdots + b_\lambda(s)\frac{d^\lambda}{ds^\lambda}M(s) = r(s) \tag{3.1}$$

with $M(s) \in \{M_1(s), \ldots, M_\lambda(s)\}$, polynomials $b_i(s)$ in s and a given right hand side $r(s)$ that is given by a linear combination in terms of the already handled master integrals. Plugging $M(s) = \sum_{n=0}^{\infty} G(n) s^n$ into this equation and performing coefficient comparison with respect to s^n leads to a linear recurrence relation

$$a_0(n)G(n) + \cdots + a_\delta(n)G(n+\delta) = R(n) \tag{3.2}$$

of some order δ with polynomials $a_i(n)$ in n where the coefficients $R(n)$ for $n < \rho$ are given explicitly.

I.3 Without loss of generality, we may assume that $a_\delta(n) \neq 0$ for all $n \geq \delta$; otherwise increase δ such that this is the case. Suppose in addition that we are given δ initial values for $G(n)$. Then we use the recurrence (3.2) to prolong the sequence $G(n)$ to $n < \rho$ in linear time with respect to the number of operations in[5] $\mathbb{Q}$.

I.4 Any of the available uncoupling algorithms from Step I.1 allows one to express the remaining unknown MIs in terms of a linear combination of the determined MIs (including their differentiated versions) from the previous step (and the already solved MIs from previous recursions). Thus expanding those expressions leads to a power series representation where the first ρ coefficients are given explicitly.

An extra complication is that the coupled system contains also the dimensional parameter ε and one is interested in a Laurent series expansion of the $M_i(\varepsilon, s)$ not only in s but but also in ε. Here two refined methods have been elaborated in Refs. [12, 99] where in both cases one ends up at a linear recurrence of the form (3.2). Depending on the choice of the strategy, the coefficients are free of ε, i.e., we simply follow Step I.3 above. If they depend on ε one may use the tools described in Ref. [100] to prolong the sequence for the different ε-contributions.

To fine-tune the large moment method, we carried out the different systems systematically by applying all the available uncoupling methods, in our case Gauß and Zürcher, and the available strategies to handle the ε-expansions in order to select the best strategy such that the order δ of the derived recurrences and the required ε-order of master integrals is minimized simultaneously; for a careful study we refer also to [101].

After applying the four steps I.1–I.4 from above iteratively to the 147 recursively defined sub-systems, one deals with the physical expression coming from the IBP reductions as carried out in Step II: one plugs in the explicitly given expansions of the master integrals up to the order ρ into the physical expression and expands it to get the first ρ coefficients of the s-expansion. Examples of the explicit expansions of the form factors F_I coming from Step II will be given in Section 4.

3.1 From few to many coefficients

In order to prolong the coefficients to the desired number ρ using the recurrence (3.2) in Step I.2, at least δ initial values have to be provided. If δ is too large[6], their direct calculation becomes computationally prohibitive. Thus keeping δ as small as possible is crucial when deriving the recurrence (3.2) from the differential equation (3.1).

Strategy 1: Minimizing the order. We leverage the fact that the order δ is bounded by (and generically equals)

$$\delta \leq \max_i \deg_s(b_i) + \lambda;$$

compare Refs. [102, 103]. To minimize δ, a straightforward approach is to reduce the degrees of the coefficients $b_i(s)$ by canceling their greatest common divisor. Further refinements from Refs. [12,99] reduced these potential orders by roughly 40, bringing the required number of initial values into a manageable computational range.

We note that minimizing the order δ is made possible by shifting the extra factors from the left-hand side of (3.1) to the denominators of the right-hand side, $r(s)$. However, this introduces

[5]We note that the size of the rational numbers grows significantly for large n, meaning arithmetic operations require non-constant time in terms of processor words. We omit a formal complexity analysis and instead provide later computation times to illustrate the computational challenge.

[6]Whereas about 20 initial values can easily be computed for simpler integrals, the task already becomes demanding at 10 values for more involved cases.

more complicated rational functions multiplying the already-evaluated master integrals. Consequently, the power series expansion of $r(s)$ required to obtain $R(n)$ for $n = 0, \ldots, \rho - 1$ becomes significantly more involved. We note that these complications could be managed for expansions up to $\rho = 12000$ using the techniques described in Ref. [95].

For the different contributions the number ρ was chosen big enough to succeed in guessing afterwards a linear recurrence/differential equation of the physical problem coming from the coefficients when performing Step II introduced above. Recursions of different complexity need input sets of different size, ranging from $\rho = 500$ to $\rho = 12000$ for all but the three cases without ζ-weights, which required about 6 months of parallel running using 10–12 processes.

However, we needed much more coefficients to handle the remaining parts. In a first attempt we calculated $\rho = 25000$ coefficients. This challenge forced us to invert the above strategy entirely.

Strategy 2: Simplifying the right-hand side. We clear all denominators in $r(s)$ by multiplying both sides by a large polynomial, which increased in the worst cases the degrees of the $b_i(s)$ up to 200. This yields a linear recurrence (3.2) with $\lambda \sim 200$. On the other side, $r(s)$ is now given as a linear combination of master integrals with simple polynomial coefficients in s (or s, ε). Consequently, expanding $r(s)$ to obtain $R(n)$ for $n = 0, \ldots, \rho - 1$ becomes significantly more efficient. Although the prolongation requires $\lambda \sim 200$ initial values and takes longer due to the larger recurrence, its complexity remains linear in the number of field operations. For instance, by taking $\rho = 25000$ this prolongation was completed in just a few hours.

Combining Strategy 1 and 2: The true strength of our method lies in combining these two approaches. First, we compute $\rho = 500$ values for the full problem within a day using the first approach, leveraging the initial values available from direct calculations. Second, we utilize these 500 coefficients as the initial values for the second approach to scale the computation up to $\rho = 25000$.

We remark that Strategy 2 can be also applied to speed up Step II: clearing denominators of the physical expression with a common huge factor $d(s, \varepsilon)$ enables one to compute the expansion in s and ε by simple polynomial arithmetic. Only in the end, one divides the found truncated polynomial by $d(s, \varepsilon)$ and computes the expansion in s and ε following the ideas presented in Ref. [95]. To compute $\rho = 25000$ coefficients of all the MIs took about 11 months.

In our original implementation of the package `SolveCoupledSystem` [12, 104, 105] implemented for `Mathematica`, standard parallelization has been treated that assumes that the appearing MIs can be stored directly in memory, a strategy that successfully sustained all our previous calculations. However, scaling up to 147 systems introduced non-trivial memory management challenges, as these systems comprise 419 MIs yielding 25,000 total values that require 5.6 TB of storage. The final values are particularly demanding, with each requiring approximately 130 kB of memory to store their 150,000 to 157,000 digits, while the right hand side of the latest systems depend on 200 to 300 MIs simultaneously. To handle the 20 most complicated systems, new computational techniques became necessary. Parallelization was distributed across multiple computers and reorganized for any given right hand side to restrict memory usage to a maximum of up to 10 MIs per `Mathematica` call. Furthermore, intermediate sub-results, which are significantly larger than the final right hand side, were written directly to hard disks, demanding meticulous coordination of disk space and subsequent manual combination. Finally, employing different uncoupling strategies, such as Gauß and Zürcher, introduced varying communication requirements that had to be partially managed through manual intervention.

3.2 Prolonging to larger coefficients

We applied the techniques described in Section 3.1 to compute $\rho = 25000$ coefficients for the constant contributions. This number proved to be sufficient to guess the required recurrence relations for all but the color factor C_F^3 for $F_{a,1}(s)$, see Eqs. (2.12) and (2.17). Rather than restarting the entire pipeline, we leveraged the existing coefficients to efficiently extend the computation to $\rho = 40000$ using the strategy outlined below, which allowed us to guess the yet missing differential equations.

(i) Using the 24000 coefficients, we guessed as many recurrence relations as possible for the 417 master integrals in 2 months of real time. For the remaining systems, only the last two ε-orders for 2 systems, and the final ε-order for 10 systems, could not be guessed.

(ii) With the successfully guessed recurrences, we generated the coefficients up to $\rho = 40000$ in about 7 days on several machines.

(iii) For the remaining 12 systems, we computed the values up to $\rho = 40000$ exclusively for the missing ε-contributions, while leveraging the lower ε-contributions obtained from the previous step. This particular calculation could not be performed in a fully automated fashion; it required manual intervention, custom job distribution of sub-problem across different machines, and meticulous memory management. In particular, intermediate results had to be strategically distributed and stored across multiple hard drives. This step amounted to 1.3 months of real run time.

In its final form, the complete dataset required approximately 5.5 TB of storage in compressed form. Combining the master integrals to extract the 40000 coefficients of C_F^3 for $F_{a,1}(s)$ took 3 weeks using parallelization. Naturally, managing these memory demands and parallelization workflows required significant additional effort compared to our previous 24000 coefficient calculations, as well as an increased level of manual intervention. The complete computation of the 40000 coefficients for the missing axial-vector contribution spanned 3.5 months running in parallel.

Ultimately, it turned out that only 26000 coefficients were strictly necessary to successfully guess the required recurrence relation.

4 Recurrences and differential equations from the low energy expansions of the form factors

The initial values for all differential equations considered in this project are given at $s = 0$, resp. $x = 1$, the low energy limit of the form factors.

Once we have computed the expansion of the master integrals at this point in Step I, we can combine them in Step II to obtain the low energy expansion of the unrenormalized form factors. In particular, we can obtain the expansions about $s = 0$ of the form factors on the right-hand side of Eqs. (2.11–2.12) and Eqs. (2.15–2.16). These expansions up to $O(\varepsilon^0)$ are of the form

$$F_I^{s\to 0}(s) = \sum_{i=-3}^{0} \varepsilon^i \sum_{j=1}^{3} C_j \sum_{k=0}^{\infty} c^{(0)}_{I;i,j,k} s^k, \tag{4.1}$$

where the color factors C_j are given in Eq. (2.18), while the coefficients $c^{(0)}_{I;i,j,k}$ are rational linear combinations of the following list of constants[7],

$$\left\{1,\, \zeta_2,\, \zeta_3,\, l_2\zeta_2,\, \zeta_2^2,\, a_4,\, l_2^4,\, l_2^2\zeta_2,\, \zeta_2\zeta_3,\, \zeta_5\right\}. \tag{4.2}$$

Using a finite but large number ρ of rational numbers, we executed an automated guessing strategy to find the underlying recurrence relations and linear differential equations.

In our specific setup, it became evident that significantly fewer coefficients were required to guess the recurrence relations than the corresponding differential equations. Consequently, we adopted a staged approach: we first guessed the recurrences, used them to generate additional coefficients, like extending 24000 initial coefficients needed for the recurrence to 40000 values needed for the differential equation. The axial-vector case stood out as an exception.

The guessing was performed using the `ore_algebra` package in `Sage`, cf. Refs. [66, 68]. For the most demanding case requiring around 25300 values to guess the linear recurrence and 37700 values to guess the linear differential equation we utilized a parallel version of the `ore_algebra` package, which was used at the supercomputer `MACH-2` at JKU to exploit 1728 processor cores and 20 TB of global shared memory. In one of the most computationally involved differential equation runs, the guessing algorithm utilized 24,420 coefficients across 800 cores, with each core computing one homomorphic image, requiring 30 hours via parallelization. Subsequently, a further optimized version of the `ore_algebra` package, allowed us to rerun this hardest case in approximately one day on a single fast workstation at RISC, parallelizing twelve times.[8]

If we rename the constants (4.2) as given in (2.23) the coefficients $c^{(0)}_{I;i,j,k}$ can be written as

$$c^{(0)}_{I;i,j,k} = \sum_{l=1}^{10} r^{(0)}_{I;i,j,l,k}\kappa_l, \tag{4.3}$$

where the $r^{(0)}_{I;,i,j,l,k}$'s are rational numbers. Introducing this equation in (4.1), we can rewrite the form factors as

$$F_I^{s\to 0}(s) = \sum_{i=-3}^{0} \varepsilon^i \sum_{j=1}^{3} C_j \sum_{l=1}^{10} \kappa_l f^{(0)}_{I;i,j,l}(s), \tag{4.4}$$

where the expansions around $s = 0$ of the functions $f_{I;i,j,l}(s)$ are given by

$$f^{(0)}_{I;i,j,l}(s) = \sum_{k=0}^{\infty} r^{(0)}_{I;i,j,l,k} s^k. \tag{4.5}$$

The differential equations obeyed by these functions and obtained through guessing algorithms will be of the form

$$p_0(s) f^{(0)}_{I;i,j,l}(s) + p_1(s)\frac{d}{ds} f^{(0)}_{I;i,j,l}(s) + p_2(s)\frac{d^2}{ds^2} f^{(0)}_{I;i,j,l}(s) + \cdots + p_r(s)\frac{d^r}{ds^r} f^{(0)}_{I;i,j,l}(s) = 0, \tag{4.6}$$

where $p_0(s)$, $p_1(s), \ldots, p_r(s)$ are polynomials in s. We will therefore have a recurrence relation and a differential equation for each one of the constants in (4.2) appearing in each color factor of each form factor. In this way, we have moved from the problem of solving differential equations obeyed by the master integrals, as it was done in Refs. [14–16, 18] and many other perturbative

[7] The label "(0)" in $c^{(0)}_{I;i,j,k}$ is used to emphasize that the expansion is around $s = 0$. We will later obtain expansions around other values of s, and the label will be changed accordingly.

[8] In the present installation we use the `Sage` linear solver `linbox_noefd`.

calculations, to the problem of solving differential equations derived from expansion coefficients. This is the same approach we used in Ref. [13] for the quarkonic case, now applied to the more involved gluonic contributions. As we will see in the next sections, this method allows us to get to such a high precision to determine the form factors in the high energy limit analytically. In earlier calculations this problem was solved purely numerically at a sufficient level of precision in Refs. [14–16, 18].

In order to guess closed-form differential equations, it is sometimes necessary to drop the first few rational numbers, which leads to inhomogeneites. This inhomogeneity can subsequently be eliminated, yielding a differential equation of the form (4.6) at the expense of increasing the order of the differential equation by one.

		ζ_2^2	$l_2^2\zeta_2$	l_2^4	a_4	$l_2\zeta_2$	ζ_3	ζ_2	1
F_s	C_F^3	14	14	14	14	33	57	59	96
	$C_A C_F^2$	14	14	14	14	33	56	57	93
	$C_A^2 C_F$	13	13	11	11	32	54	55	90
F_p	C_F^3	13	13	12	12	33	56	58	96
	$C_A C_F^2$	14	14	13	13	33	54	56	92
	$C_A^2 C_F$	11	11	9	9	30	49	51	85
$F_{v,1}$	C_F^3	14	14	13	13	36	58	60	101
	$C_A C_F^2$	14	14	13	13	36	58	61	100
	$C_A^2 C_F$	14	14	12	12	35	58	58	95
$F_{v,2}$	C_F^3	14	14	13	13	34	57	59	98
	$C_A C_F^2$	14	14	13	13	34	57	59	97
	$C_A^2 C_F$	14	14	12	12	34	55	56	92
$F_{a,1}$	C_F^3	14	14	14	14	36	58	62	102
	$C_A C_F^2$	14	14	14	14	36	58	62	101
	$C_A^2 C_F$	14	14	12	12	35	58	59	96
$F_{a,2}$	C_F^3	13	13	12	12	33	56	58	96
	$C_A C_F^2$	14	14	13	13	33	54	56	92
	$C_A^2 C_F$	11	11	9	9	30	49	51	85

Table 1: Orders of the differential equations obtained from the rational coefficients for the different color factors and different constants in (4.2) for each form factor (after removing inhomogeneities, if needed). In the case of the weight w = 5 constants, $\zeta_2\zeta_3$ and ζ_5, the orders are always equal to 2.

The recursion relations can now be used to generate a much larger amount of rational numbers in Eq. (4.5). We derived 100000 such rational numbers for all of the constants in (4.2), for each form factor and color factor. This allowed us to evaluate the functions $f^{(0)}_{I;i,j,l}(s)$ with extremely high precision within their radius of convergence, which is important for the next steps.

All pole terms obey first order factorizing difference equations. Using the recurrence solver in the setting of difference rings [72–86] of the summation package `Sigma` [69,70], all coefficients can be expressed in terms of cyclotomic harmonic sums [106]. Using the package `HarmonicSums` [87, 88] their power series representations can be rewritten in terms of harmonic polylogarithms in x, [107], or in Mellin space in harmonic sums [108, 109].

At $O(\varepsilon^0)$, the differential equations are first-order factorizable in the case of the constants ζ_5 and $\zeta_2\zeta_3$. For the remaining constants in (4.2), the differential equations are not first-order factorizable.

The degree of the polynomials and the order r of the differential equations (4.6) will in general depend on the values of I, i, j and l. In Table 1, the orders r of the differential equations obtained for the constants in (4.2) for each color factor and each form factor are given, after inhomogeneities were removed. In Table 2 we show the corresponding highest degrees of the polynomials.

		ζ_2^2	$l_2^2\zeta_2$	l_2^4	a_4	$l_2\zeta_2$	ζ_3	ζ_2	1
F_s	C_F^3	202	202	200	200	1045	1447	1434	3708
	$C_A C_F^2$	204	204	200	200	1047	1420	1379	3544
	$C_A^2 C_F$	187	187	147	147	989	1324	1297	3248
F_p	C_F^3	179	179	166	166	1057	1429	1428	3712
	$C_A C_F^2$	198	198	183	183	1065	1353	1316	3419
	$C_A^2 C_F$	139	139	95	95	875	1081	1083	2756
$F_{v,1}$	C_F^3	216	216	201	201	1210	1537	1531	4033
	$C_A C_F^2$	218	218	201	201	1212	1553	1547	3978
	$C_A^2 C_F$	212	212	160	160	1127	1468	1407	3613
$F_{v,2}$	C_F^3	194	194	181	181	1072	1448	1450	3814
	$C_A C_F^2$	196	196	181	181	1074	1447	1448	3762
	$C_A^2 C_F$	190	190	152	152	1052	1367	1338	3428
$F_{a,1}$	C_F^3	216	216	214	214	1208	1549	1570	4078
	$C_A C_F^2$	218	218	214	214	1210	1552	1568	4026
	$C_A^2 C_F$	212	212	172	172	1127	1472	1440	3684
$F_{a,2}$	C_F^3	179	179	166	166	1057	1429	1428	3712
	$C_A C_F^2$	198	198	183	183	1065	1353	1316	3419
	$C_A^2 C_F$	139	139	95	95	1081	1081	1083	2756

Table 2: Highest degrees of the polynomials appearing in the differential equations obtained from the rational coefficients for the different color factors and different constants in (4.2) for each form factor (after removing inhomogeneities, if needed). In the case of the constants $\zeta_2\zeta_3$ and ζ_5, these degrees are all equal to 6.

The singular points of the differential equations also depend on the choice of constant in (4.2). The differential equations associated to the weight $\mathsf{w} = 4$ constants have real valued singularties at $s = 0$, $s = -1$, $s = -4$, $s = 3$ and $s = 4$. In the case of $l_2\zeta_2$, in addition to the previous ones, we have also singularities at $s = -1/2$ and $s = 1$, while in the case of ζ_3, we must add a singularity at $s = 16$, and in the cases of ζ_2 and $\kappa_1 = 1$, also a singularity at $s = 16/3$ pops up. In total, there are five singularities in the case of ζ_2^2, $l_2^2\zeta_2$, l_2^4 and a_4, seven singularities in the case of $l_2\zeta_2$, eight singularities for ζ_3, and nine singularities in the cases of ζ_2 and $\kappa_1 = 1$. Of all these singularities, only the ones at $s = 4$ and $s = 16$ are physical, corresponding to the two-particle threshold and four-particle pseudo-threshold, respectively.[9] The remaining singularities are spurious, and arise only as a consequence of having split the form factors in terms of the functions $f^{(0)}_{I;i,j,l}(s)$ associated to the constants in (4.2). After we combine everything in (4.4), these spurious singularities disappear.

The simplest expansions for the form factors are obtained in the limit $s \to 0$. According to

[9] All the contributing differential equations have as well a singularity as $s \to \infty$.

Eqs. (4.4) and (4.5), the $O(\varepsilon^0)$ parts of the unrenormalized form factors are given by

$$F_I^{s\to 0}(s) = \sum_{j=1}^{3} C_j \sum_{l=1}^{10} \kappa_l f^{(0)}_{I;0,j,l}(s) = \sum_{j=1}^{3} C_j \sum_{l=1}^{10} \sum_{k=0}^{\infty} r^{(0)}_{I;0,j,l,k} \kappa_l s^k, \tag{4.7}$$

where the C_j's are the color factors given in Eq. (2.18), while the coefficients $r^{(0)}_{I;0,j,l,k}$ are rational numbers.

Before we show an explicit example of such an expansion, we should talk about the solvable parts of the form factors. For two of the constants in Eq. (2.23), namely, $\kappa_9 = \zeta_2\zeta_3$ and $\kappa_{10} = \zeta_5$, the corresponding differential equations in the variable x for the functions $f_{I;0,j,l}(s)$ in Eq. (4.4) were solved analytically. As might have been expected, due to the high transcendentality of these constants, the solutions turned out to be very simple, depending only on $\ln(x)$ and rational functions in x. In the vector case, setting $N_c = 3$, for the corresponding contributions to $F_{v,1}(s)$ at $O(\varepsilon^0)$ we obtained

$$\begin{aligned}\sum_{j=1}^{3} C_j \sum_{l=9}^{10} \kappa_l f_{v,1;0,j,l}(s) &= 64\Bigg\{-\zeta_2\zeta_3\left(\frac{2018 - 7743x - 3634x^2 - 7743x^3 + 2018x^4}{27(1-x)x(1+x)}\ln(x)\right.\\ &\quad\left.+\frac{1703 - 8712x + 1703x^2}{9x}\right) + \zeta_5\left(\frac{4313 - 27032x + 4313x^2}{108x}\right.\\ &\quad\left.\left.-\frac{5\,(502 - 2041x + 2196x^2 - 2041x^3 + 502x^4)}{54(1-x)x(1+x)}\ln(x)\right)\right\},\end{aligned} \tag{4.8}$$

while the corresponding contributions to $F_{v,2}(s)$ are given by[10]

$$\begin{aligned}\sum_{j=1}^{3} C_j \sum_{l=9}^{10} \kappa_l f_{v,2;0,j,l}(s) &= 64\Bigg\{-\zeta_2\zeta_3\left(\frac{2018 + 3940x + 5773x^2 + 3940x^3 + 2018x^4}{54(1-x)x(1+x)}\ln(x)\right.\\ &\quad\left.+\frac{26561 + 49264x + 26561x^2}{216x}\right) + \zeta_5\left(\frac{13801 + 25072x + 13801x^2}{432x}\right.\\ &\quad\left.\left.-\frac{5\,(502 + 1028x + 799x^2 + 1028x^3 + 502x^4)}{108(1-x)x(1+x)}\ln(x)\right)\right\}.\end{aligned} \tag{4.9}$$

The poles in ε in Eq. (4.4) can also be solved exactly as functions of x. However, the resulting expressions are generally considerably more involved than those in Eqs. (4.8–4.9), with their complexity increasing with the order in ε. The $O(\varepsilon^{-3})$ terms have a structure similar to that of the results above, being expressed solely in terms of $\ln(x)$ and rational functions of x. At $O(\varepsilon^{-2})$, harmonic polylogarithms of weight up to $\mathsf{w} = 3$ appear, whereas the $O(\varepsilon^{-1})$ terms involve harmonic polylogarithms of weight up to $\mathsf{w} = 5$.

The exact solutions in x for the $\zeta_2\zeta_3$ and ζ_5 contributions at $O(\varepsilon^0)$, such as those given in Eqs. (4.8)–(4.9), together with the exact solutions for the poles in ε, are valid throughout the entire kinematic range[11]. They can therefore be expanded about any value of s, including $s = 0$, by using Eq. (1.3).

When reconstructing the form factors $F_{V,1}(s)$ and $F_{V,2}(s)$ from Eq. (2.11), or $F_{A,1}(s)$ and $F_{A,2}(s)$ from Eq. (2.12), it is important to take into account that the projector coefficients

[10] The corresponding expressions for the other form factors are given in an ancillary file.

[11] For this reason we removed the labels "(0)" or "(s_0)" from $f_{I;0,j,l}(s)$ in Eqs. (4.8)–(4.9)

$g_{I,i}^{(k)}$ in Eqs. (2.7–2.10) depend on ε. Consequently, after expanding these coefficients in ε, the contributions of order $O(\varepsilon^i)$ with $i \leq 0$ contribute to the finite, $O(\varepsilon^0)$, terms.

As an illustrative example, we present the expansion of the vector current form factor $F_{V,1}(s)$ up to $O(s^5)$. It is obtained by combining the expansions of the non-solvable contributions in Eq. (4.4), corresponding to the constants κ_l with $1 \leq i \leq 8$ in Eqs. (2.23), with the expansions of the exact $\zeta_2\zeta_3$ and ζ_5 solutions, together with the contributions originating from the poles in ε. Setting again $N_c = 3$, we obtain

$$
\begin{aligned}
F_{V,1}^{s\to 0} = \\
&64\Bigg\{\frac{274321}{324}+\frac{589477}{2592}\zeta_2+\frac{3679}{27}l_2\zeta_2-\frac{619}{18}l_2^2\zeta_2+\frac{28873}{1440}\zeta_2^2-\frac{3079}{108}\zeta_3-\frac{349}{9}\zeta_2\zeta_3+\frac{713}{27}\zeta_5\\
&-\frac{2099}{27}a_4-\frac{2099}{648}l_2^4+s\Bigg[-\frac{30176683}{139968}+\frac{658}{27}a_4+\frac{329}{324}l_2^4-\frac{1381189}{139968}\zeta_2\\
&-\frac{31435}{648}l_2\zeta_2+\frac{350}{27}l_2^2\zeta_2+\frac{41711}{2430}\zeta_2^2+\frac{258683}{11664}\zeta_3-\frac{905}{108}\zeta_2\zeta_3-\frac{1165}{432}\zeta_5\Bigg]\\
&+s^2\Bigg[-\frac{188800077257}{2799360000}+\frac{104717}{12150}a_4+\frac{104717}{291600}l_2^4-\frac{17227423687}{4898880000}\zeta_2\\
&-\frac{181845473}{13608000}l_2\zeta_2+\frac{315487}{85050}l_2^2\zeta_2-\frac{43819}{272160}\zeta_2^2+\frac{935160107}{124416000}\zeta_3-\frac{7507}{6480}\zeta_2\zeta_3-\frac{53}{144}\zeta_5\Bigg]\\
&+s^3\Bigg[-\frac{75271254677139169}{3629482214400000}+\frac{1053107}{297675}a_4+\frac{1053107}{7144200}l_2^4-\frac{566793123524251}{221801690880000}\zeta_2\\
&-\frac{6736570381}{2000376000}l_2\zeta_2+\frac{623204}{297675}l_2^2\zeta_2-\frac{9668233}{9525600}\zeta_2^2+\frac{4449995721067}{1536288768000}\zeta_3-\frac{10711}{90720}\zeta_2\zeta_3\\
&-\frac{3293}{36288}\zeta_5\Bigg]+s^4\Bigg[-\frac{1532491738898017906343}{200695848527462400000}+\frac{228437}{238140}a_4+\frac{228437}{5715360}l_2^4\\
&-\frac{5429386088673075803}{1245638295982080000}\zeta_2+\frac{1669776162077}{422479411200}l_2\zeta_2+\frac{1963141}{17463600}l_2^2\zeta_2-\frac{7147363}{75442752}\zeta_2^2\\
&+\frac{48280096513375243}{28316874571776000}\zeta_3+\frac{653}{45360}\zeta_2\zeta_3-\frac{263}{9072}\zeta_5\Bigg]+s^5\Bigg[-\frac{4100027832392971406645049 7}{16454972342427231191040000}\\
&+\frac{1529009641}{2593344600}a_4+\frac{1529009641}{62240270400}l_2^4-\frac{6157090135300397592929177}{2142064386962175836160000}\zeta_2\\
&+\frac{63096225504033647}{19936803414528000}l_2\zeta_2+\frac{39051357271}{67426959600}l_2^2\zeta_2-\frac{104412436391}{299675376000}\zeta_2^2\\
&+\frac{23806175381893363619}{21537005745733632000}\zeta_3+\frac{23207}{1496880}\zeta_2\zeta_3-\frac{977}{99792}\zeta_5\Bigg]\Bigg\}+O(s^6). \qquad (4.10)
\end{aligned}
$$

5 Expansions at other points by analytic continuation

We can now use the expansions around $s = 0$, for the differential equations of all form factors for each constant in these expansions, to compute the corresponding expansion at other points in s. Main targets are the expansions in the high energy limit $s \to \infty$, at the two-particle threshold

($s = 4$), and the four-particle pseudo-threshold ($s = 16$). The expansions at other points are also important for two reasons:

1. The calculation of these expansions are needed as intermediate steps to reach these points.

2. They are needed for accurate numerical evaluations of the form factors in the whole kinematic range $-\infty < s < +\infty$.

We will determine the coefficients of these expansions numerically with very high precision such that it will be sufficient to express the coefficients of the expansions around $s \to \infty$ in terms of special constants, as, e.g. multiple zeta values [62] and others, using the PSLQ algorithm [110–112], after a number of necessary matchings.

The radius of convergence of the expansions about $s = 0$ depends on the constant in (4.2) under consideration, since the location of the nearest singularity is constant dependent. For the weight $\mathsf{w} = 4$ constants, the closest singularity is located at $s = -1$, whereas for the remaining constants, it is at $s = -1/2$. To generate expansions about negative values of s, we may begin by choosing either a regular point between $s = 0$ and the nearest singularity or the singular point itself as the center of the next expansion.

The basic idea of the method is to determine the coefficients of the expansion about the new point numerically by matching it to the expansion about $s = 0$ within their common region of convergence. This procedure can then be iterated, constructing a sequence of expansions at progressively more negative values of s, with each new expansion matched to the preceding one. The same strategy is applied for positive values of s. In this way, the analytic continuation is carried out across the entire real axis, including through the singular points. Once a sufficiently large positive or negative value of s has been reached, the corresponding expansion can be matched to the asymptotic expansion at $s \to \infty$. A corresponding calculation in Refs. [14–19] has been performed directly to the coupled systems of the master integrals by using the Frobenius method. For a general survey including existence results and also error bounds we refer, e.g., to [113–115] and references therein.

5.1 The structure of the local expansions at the different points of interest

Since the poles in ε of all form factors can be obtained in terms of known functions, the method we are about to describe will only be applied to the $O(\varepsilon^0)$ terms. Therefore, we drop the index $i = 0$ in the functions $f^{(0)}_{I;i,j,l}(s)$, and simply write $f^{(0)}_{I;j,l}(s)$. Furthermore, we replace the label "(0)" by "(s_0)" to indicate that the expansions are now about $s = s_0$ instead of $s = 0$. For regular points, the expansions will have the following form

$$f^{(s_0)}_{I;j,l}(s) = \sum_{k=0}^{\infty} b^{(s_0)}_{I;j,l,k} z^k, \tag{5.1}$$

where $z = s - s_0$. For $s_0 \neq 0$, the coefficients $b^{(s_0)}_{I;j,l,k}$ will not necessarily be real, but also complex numbers.

Around singular points, the expansions may include powers of logarithms and negative powers in z, and the relation between z and s may involve square roots. All of this can be determined by studying the differential equations. In general, the expansions at the singular points, assuming that we are considering a constant κ_l such that the point is indeed singular. A series of representations is

$$f^{(-1/2)}_{I;j,l}(s) = \sum_{k=0}^{\infty}\sum_{i=0}^{1} b^{(-1/2)}_{I;j,l,i,k} z^k \ln^i(z), \quad \text{with} \quad z = s + 1/2, \tag{5.2}$$

$$f^{(-1)}_{I;j,l}(s) = \sum_{k=-3}^{\infty} b^{(-1)}_{I;j,l,k} z^k, \quad \text{with} \quad z = \sqrt{1+s}, \tag{5.3}$$

$$f^{(-4)}_{I;j,l}(s) = \sum_{k=-2}^{\infty}\sum_{i=0}^{2} b^{(-4)}_{I;j,l,i,k} z^k \ln^i(z), \quad \text{with} \quad z = s + 4, \tag{5.4}$$

$$f^{(1)}_{I;j,l}(s) = \sum_{k=-6}^{\infty}\sum_{i=0}^{1} b^{(1)}_{I;j,l,i,k} z^k \ln^i(z), \quad \text{with} \quad z = s - 1, \tag{5.5}$$

$$f^{(3)}_{I;j,l}(s) = \sum_{k=-3}^{\infty} b^{(3)}_{I;j,l,k} z^k, \quad \text{with} \quad z = \text{sign}(3-s)\sqrt{3-s}, \tag{5.6}$$

$$f^{(4)}_{I;j,l}(s) = \sum_{k=-5}^{\infty}\sum_{i=0}^{3} b^{(4)}_{I;j,l,i,k} z^k \ln^i(z), \quad \text{with} \quad z = \text{sign}(4-s)\sqrt{4-s}. \tag{5.7}$$

$$f^{(16)}_{I;j,l}(s) = \sum_{k=0}^{\infty} b^{(16)}_{I;j,l,k} z^k, \quad \text{with} \quad z = -i\sqrt{s-16}. \tag{5.8}$$

Likewise, the expansion at $s \to \infty$ is given by

$$f^{(\infty)}_{I;j,l}(s) = \sum_{k=-4}^{\infty}\sum_{i=0}^{6} b^{(\infty)}_{I;j,l,i,k} z^k \ln^i(z), \quad \text{with} \quad z = \sqrt{-\frac{1}{s}}. \tag{5.9}$$

In these equations, the lowest allowed values of k and the highest powers of the logarithms are determined by the differential equations, considering all values of j and l for all form factors. In some cases, the starting value of k is higher; in such cases, the corresponding coefficient $b^{(s_0)}_{I;j,l,i,k}$ is set to zero.

The full form factors can be written at $O(\varepsilon^0)$ in a similar way as in Eq. (4.4),

$$F^{(s_0)}_I(s) = \sum_{j=1}^{3} C_j \sum_{l=1}^{10} \kappa_l f^{(s_0)}_{I;j,l}(s). \tag{5.10}$$

After combining all terms in Eq. (5.10), all logarithms and square roots disappear around the spurious singular points $s = -1/2, -1, -4, 1, 3$, and we are left with ordinary expansions about these points like the ones in Eq. (5.1). In the case of the expansions at infinity, the logarithms remain, but the square roots disappear, and we end up with an asymptotic expansion in $-1/s$, see Section 6.

The set of expansion points must include the singular points of the differential equations. Beyond this, there is considerable freedom in the choice of regular expansion points. For the weight $\mathsf{w} = 4$ constants in (4.2), and for $s < 0$, we chose the following set of expansion points,

$$s_0 \in \{-196,\, -100,\, -52,\, -28,\, -16,\, -10,\, -7,\, -4,\, -3,\, -2,\, -1\}\,. \tag{5.11}$$

This choice is motivated by the radii of convergence associated with the different expansion points. Since the expansions are matched sequentially, each successive expansion point in the

negative direction is chosen to lie on the boundary of the radius of convergence of the preceding one, as illustrated in Figure 2. This strategy maximizes the overlap between the regions of convergence of consecutive expansions, thereby facilitating the matching procedure. For example, since the radius of convergence of the expansions at $s = -4$ is equal to 3 (the nearest singularity is at $s = -1$), the next expansion point is chosen at $s = -7$. The expansion at $s = -7$ also has a radius of convergence equal to 3 (nearest singularity at $s = -4$), so the next expansion is at $s = -10$, which has a radius of convergence equal to 6, so the next expansion is chosen at $s = -16$.

Similar illustrations apply to the convergence circles of the other expansion points in s. For $s > 0$, we chose

$$s_0 \in \{1,\, 2,\, 3,\, 4,\, 5,\, 6,\, 8,\, 12,\, 16\}\,. \tag{5.12}$$

The expansions about $s = 1, 2, 3$ were constructed sequentially to reach the two-particle threshold at $s = 4$.

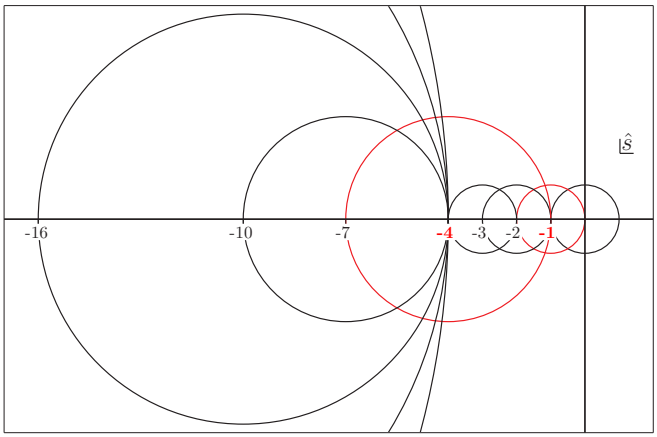

Figure 2: Radii of convergence of the successive points around which expansions are matched in the case of the weight w = 4 constants for $s < 0$. The points $s = -1$ and $s = -4$, shown in red, are singularities of the differential equations, which disappear after everything is combined in Eq. (5.10).

The expansion about $s = 16$, corresponding to the four-particle pseudo-threshold, was instead obtained by matching directly to the expansion around $s \to \infty$. Consequently, the intermediate expansion points at $s = 5, 6, 8, 12$, are not strictly required for this construction. Nevertheless, we computed these additional expansions to enable an efficient numerical evaluation of the form factors with very high precision over the entire kinematic region.

In the case of the constant $\kappa_4 = l_2\zeta_2$, we also have singularities about $s = -1/2$ and $s = -1$. Therefore, for this constant we chose the following expansion points for $s < 0$,

$$s_0 \in \left\{-196,\, -100,\, -52,\, -28,\, -16,\, -10,\, -7,\, -4,\, -3,\, -2,\, -\frac{3}{2},\, -1,\, -\frac{1}{2}\right\}. \tag{5.13}$$

For $s > 0$, we adopted a slightly different strategy from that based solely on the radii of convergence. Instead, we performed expansions around every integer and half-integer value of s up to $s = 4$. The complete set of expansion points is

$$s_0 \in \left\{\frac{1}{2},\, 1,\, \frac{3}{2},\, 2,\, \frac{5}{2},\, 3,\, \frac{7}{2},\, 4,\, 5,\, 6,\, 8,\, 12,\, 16\right\}. \tag{5.14}$$

The inclusion of these additional intermediate expansion points improves the numerical precision of the matching procedure, since shorter matching steps reduce the accumulation of numerical errors.

In the case of the constants $\kappa_1 = 1$, $\kappa_2 = \zeta_2$ and $\kappa_3 = \zeta_3$, the expansion points in (5.13) and (5.14) were not enough to achieve sufficiently high precision. Therefore, in the case of these constants, we included expansion points in middle of each pair of points in (5.13) and each pair of points in (5.14) up to $s = 4$, since, as we already mentioned in the case of $l_2\zeta_2$, the more points we include, the higher the precision that can be achieved. For $s < 0$, we then have

$$\begin{aligned} s_0 \in \Big\{ & -196, -148, -100, -76, -52, -40, -28, -22, -16, -13, -10, -\frac{17}{2}, -7, -\frac{11}{2}, \\ & -4, -\frac{7}{2}, -3, -\frac{5}{2}, -2, -\frac{7}{4}, -\frac{3}{2}, -\frac{5}{4}, -1, -\frac{3}{4}, -\frac{1}{2}, -\frac{1}{4} \Big\}, \end{aligned} \tag{5.15}$$

while for $s > 0$, we chose

$$s_0 \in \left\{ \frac{1}{4}, \frac{1}{2}, \frac{3}{4}, 1, \frac{5}{4}, \frac{3}{2}, \frac{7}{4}, 2, \frac{9}{4}, \frac{5}{2}, \frac{11}{4}, 3, \frac{13}{4}, \frac{7}{2}, \frac{15}{4}, 4, 5, 6, 8, 12, 16 \right\}. \tag{5.16}$$

It is worth noting that, in the case of the constants $\kappa_1 = 1$ and $\kappa_2 = \zeta_2$, the differential equations exhibit a singularity at $s = 16/3$. To avoid this singular point during the matching procedure, we obtain the expansions around $s = 5$ by matching them directly to the expansions around $s = 4$. The expansions around $s = 6$, $s = 8$, and $s = 12$ are instead obtained in the reverse direction: the expansions around $s = 16$ (which can themselves be determined by matching to the expansions at $s \to \infty$) are matched to the expansions around $s = 12$, which are subsequently matched to those around $s = 8$ and $s = 6$.

5.2 Computing the expansion at the individual points

When carrying out the analytic continuation starting at $s = 0$, it was necessary to compute a basis of the truncated series solutions at the individual points up to a high order N. In the following, we focus on variants of the computation implemented in the new `Mathematica` package `HolonomicContinuation`[12] with a special focus on computer algebra tools to deal with huge differential equations.

The differential equations in s can be transformed into differential equations in $z = s - s_0$, both for singular and regular points (see (5.1)–(5.9)), using the corresponding change of variables to get a differential equation

$$a_0(z)F(z) + a_1(z)\frac{d}{dz}F(z) + \cdots + a_r(z)\frac{d^r}{dz^r}F(z) = 0 \tag{5.17}$$

with polynomials $a_i(z)$ in z and rational number coefficients. The general expansion in z for the form factors have then the following shape:

$$F(z) = \sum_{i=0}^{k} \ln^i(z) \sum_{j=l}^{\infty} c_i(j) z^j \text{ with } l \in \mathbb{Z} \text{ and } c_i(j) \in \mathbb{Q}. \tag{5.18}$$

[12]The freely available package `HolonomicContinuation` can be downloaded from `https://risc.jku.at/sw/HolonomicContinuation/`.

5.2.1 Log-free contributions

In the case of regular points, substituting the corresponding series expansion (5.1) with $z = s - s_0$ into these differential equations yields relations among the coefficients $b^{(s_0)}_{I;j,l,k}$. As a result, all coefficients can be expressed in terms of a finite set of independent coefficients, whose number is equal to the order of the differential equation.

As an illustrative example, consider the pseudoscalar function $f^{(-2)}_{p;3,7}(s)$, corresponding to the color factor $C_3 = C_A^2 C_F$ and the constant $\kappa_7 = l_2^4$. Its expansion is given by Eq. (5.1), with $s_0 = -2$. Substituting this expansion into the corresponding differential equation in z, which is of order 9, see Table 1, reveals that the first 9 coefficients,

$$\left\{ b^{(-2)}_{p;3,7,0} \, , \, b^{(-2)}_{p;3,7,1} \, , \cdots , b^{(-2)}_{p;3,7,8} \right\} , \tag{5.19}$$

form a set of independent coefficients. All subsequent coefficients are expressed as linear combinations of those over explicitly given rational numbers.

We can similarly obtain relations between the coefficients when the change of variables from s to z involves a square root. In the log-free case, this can occur only at the singular points $s = -1$, $s = 3$, and $s = 16$, see Eqs. (5.3), (5.6) and (5.8). For example, consider the pseudoscalar function $f^{(-1)}_{p;1,5}(s)$, corresponding to the color factor $C_1 = C_F^3$ and the constant $\kappa_5 = \zeta_2^2$. Its expansion is given by Eq. (5.3). Substituting this expansion into the corresponding differential equation in z, which is of order 13, cf. Table 1, one finds that every coefficient in the series can be expressed as a rational linear combination of the following 13 independent coefficients:

$$\begin{aligned} \Big\{ & b^{(-1)}_{p;1,5,-1} \, , \, b^{(-1)}_{p;1,5,0} \, , \, b^{(-1)}_{p;1,5,2} \, , \, b^{(-1)}_{p;1,5,4} \, , \, b^{(-1)}_{p;1,5,6} \, , \, b^{(-1)}_{p;1,5,8} \, , \, b^{(-1)}_{p;1,5,10} \, , \\ & b^{(-1)}_{p;1,5,12} \, , \, b^{(-1)}_{p;1,5,14} \, , \, b^{(-1)}_{p;1,5,16} \, , \, b^{(-1)}_{p;1,5,18} \, , \, b^{(-1)}_{p;1,5,20} \, , \, b^{(-1)}_{p;1,5,22} \Big\} . \end{aligned} \tag{5.20}$$

Note that the coefficients of z with odd powers depend only on $b^{(-1)}_{p;1,5,-1}$. One has

$$b^{(-1)}_{p;1,5,1} = \frac{9}{40} b^{(-1)}_{p;1,5,-1} \tag{5.21}$$

$$b^{(-1)}_{p;1,5,3} = \frac{14489}{960} b^{(-1)}_{p;1,5,-1} \tag{5.22}$$

$$b^{(-1)}_{p;1,5,5} = \frac{55417}{25600} b^{(-1)}_{p;1,5,-1} \tag{5.23}$$

$$\vdots \; = \; \vdots$$

The coefficients multiplying even powers of z, on the other hand, are rational linear combinations of the independent even-power coefficients listed in Eq. (5.20). The rational coefficients rapidly acquire extremely large numerators and denominators. Their size increases significantly for coefficients of higher powers, making exact symbolic manipulations increasingly demanding. This approach remains feasible in cases where the number of coefficient relations required to achieve the desired numerical precision is not too large, such as for the weight $\mathsf{w} = 4$ constants and the $l_2\zeta_2$ contribution. For the cases $\kappa_1 = 1$, $\kappa_2 = \zeta_2$, and $\kappa_3 = \zeta_3$, however, substantially more coefficient relations are needed, making the direct symbolic approach impractical.

We consider here the case (5.18) with $k = 0$ and $l = 0$, i.e., for log-free series expansions of the form

$$F(z) = \sum_{j=0}^{\infty} c(j) z^j \text{ with } c(j) \in \mathbb{Q}. \tag{5.24}$$

We employ an improved procedure to determine r linearly independent (truncated) power series solutions (which can be expressed by r free parameters). Plugging (5.24) into (5.17) and performing coefficient comparison with respect to z^j yields a recurrence for the coefficients $c(j)$ of the series solutions of the form

$$b_0(j)c(j) + b_1(j)c(j+1) + \cdots + b_u(j)c(j+u) = 0 \tag{5.25}$$

for some polynomials $b_i(j)$ in j.

For the differential equation (5.17) of order r coming from the substitution $s - s_0 \to z$, it suffices to give $F(z)$ up to order $r-1$ to uniquely determine the full solution $F(z)$. To get a basis of all truncated series solutions we set as initial terms $F_i(z) = \sum_{j=0}^{r-1} \delta_i(j) z^j$ for $0 \leq i < r$, where $\delta_i(j)$ is 1 if $j = i$ and 0 otherwise. By using the recurrence (5.25), we prolong $F_i(s)$ for each i up to z^N for some large $N \in \mathbb{N}$. At first glance, if the order u of the recurrence is larger than r, more initial terms are needed to get a similar statement for the sequences which are a solution of the recurrence. However, note that the sequence $c(j)$ can be trivially extended to $-\infty$ be setting $c(j) = 0$ for $j < 0$. Furthermore, by Theorem 3.5, Ref. [102], the full two-sided sequence $(c(j))_{j\in\mathbb{Z}}$ is a solution of the recurrence. That is, we extend the initial values $c(0), \ldots, c(r-1)$ to $c(j)$ for $u - r \leq j < r$ and can compute $c(r), \ldots, c(N)$ using the recurrence.

For the substitution $\sqrt{s - s_0} \to z$ one needs to split the problem between the even and the odd cases accordingly. As shown in the example given above for (5.3), we determine the free coefficients in advance by naive linear system solving and proceed accordingly to obtain r linearly independent (truncated) power series solutions in z as described previously.

For the constant $\kappa_1 = 1$, carrying out this computation in reasonable time was especially challenging for the following reasons:

1. The coefficients of the polynomials in the differential equations are very large, sometimes more than 10000 digits.

2. The order and the degree of the differential equations are very large, up to 102 and 4078, respectively, see Tables 1 and 2. Therefore, also the order and the degree of the associated recurrences, which are obtained using closure properties, are very large, up to 4078 and 102.

3. The obtained recurrences are numerically ill-conditioned. That is, even if very precise approximations for $c(k), \ldots, c(k+u-1)$ are supplied to the recurrence, the computed values $\tilde{c}(k+u), \tilde{c}(k+u+1), \ldots$ lose precision very quickly.

Note that it is not necessary to compute the exact values $c(0), \ldots, c(N) \in \mathbb{Q}$. Precise approximations are sufficient. However, due to the third reason mentioned above, doing the computation numerically was not feasible, and the entire calculation of the truncated series solutions had to be performed using exact numbers.

The enormous size of the recurrences made the computation using rational numbers very expensive, which is why we chose a different approach. Instead of directly computing the $c(j) \in \mathbb{Q}$, we first compute $c(j)$ modulo several (machine-sized) primes. Then we use the Chinese Remainder Theorem and rational number reconstruction [116], to retrieve the exact $c(j) \in \mathbb{Q}$. For maximal performance, we implemented this in C using the C-library `FLINT` [117]. This approach turned out to be more than 25 times[13] faster than our best implementation based on pure rational number arithmetic. For an efficient implementation, the following three observations were crucial:

[13]Here we compared with our first implementation in `FLINT`, which was based on pure rational number arithmetic (using the same algorithm) for C_1 and $\kappa_1 = 1$, i.e., $f_{s;1,1}(s)$ for 15000 values. (4 vs. 101 CPU-hours)

1. Since the computation time in this approach is dominated by the evaluation of the polynomials of the recurrence, it is important to handle all r elements in the basis of truncated series solutions at the same time. In this way the polynomials have to be evaluated only once for each prime.

2. The denominator of consecutive values $\mathrm{den}(c(j))$ and $\mathrm{den}(c(j+1))$ are very similar, that is, the quotient of these denominators is a rational number of small size. So for reconstructing $c(j+1)$, one can multiply the computed modular images $c(j+1) \mod p$ with $\mathrm{den}(c(j))$ and then reconstruct $\mathrm{den}(c(j))\, c(j+1)$. With this approach, only about half as many primes are needed, since we observed that in our case $\mathrm{den}(c(j))c(j+1)$ has about half the size (half the number of digits) as $c(j+1)$.

3. Note that the size of $c(j)$ increases approximately linearly in j, so if $j_1 < j_2$, then less primes are sufficient for reconstructing $c(j_1)$ than for $c(j_2)$. If the reconstruction succeeded already for $c(M-u+1), \ldots, c(M) \in \mathbb{Q}$ for some $M > u$, then these values can be used as new initial values for next primes to compute $c(M+1), c(M+2)$, etc.

To save memory, the final result is transformed from exact rational numbers to a numerical representations with up to 5000 digits.

The above approach for power series expansions (5.24) in z can be extended straightforwardly to Laurent series expansions with $l \in \mathbb{Z}$.

5.2.2 Expansions with log-contributions

Finally, we consider the general case of our form factor calculation having expansions of the form (5.18) with $k \geq 1$. The most involved situation appeared with $k = 6$ at the point $s \to \infty$. For simplicity, we restrict (5.18) to $l = 0$. For this particular case, we need to compute a basis of the truncated versions of solutions of the form

$$F(z) = \sum_{i=0}^{k} \ln^i(z) \sum_{j=0}^{\infty} c_i(j) z^j \text{ and } c_i(j) \in \mathbb{Q}. \tag{5.26}$$

As in the log-free situation, exactly r values $c_i(j)$ uniquely determine all the other coefficients; however, they distribute over the different log-contributions.

To handle this situation, we determine in a preprocessing step the initial values by plugging in the ansatz (5.26), matching coefficients for $\ln^i(z) z^j$ for $i = 0, \ldots, k$ and $j = 0 \ldots, \rho$ and deriving $(k+1)\rho$ constraints in $(k+1)\rho$ unknowns; if $s - s_0 \to z$ we can take $\rho = r$, and if $\sqrt{s - s_0} \to z$ we take $\rho = 2r$.[14] Solving for this system enables one to express the $(k+1)\rho$ coefficients by a linear combination of r unknowns. In the generic case, we found that the $c_i(j)$ for $0 \leq j < n_i$ with $n_i \geq 1$ and $n_0 + \cdots + n_k = \rho$ remain free and the other coefficients are determined linearly by them.

Remark. In the largest case (the constant case κ_1 with expansions around ∞), the order of the differential equations was $r = 102$ and $k = 6$. Due to technical reasons we had to set even $r = 140$, i.e., had to solve linear systems of sizes around 1000×1000. To perform this efficiently, the solutions of the linear system has been obtained by solving the system modulo several (machine-sized) primes, using the Chinese Remainder Theorem and rational number reconstruction.

[14] Usually, we set ρ to be larger than the order of the given differential equation to handle the pole situation arising from the underlying recurrence.

With this data, we proceeded as follows to compute the first $N+1$ coefficients of the r linearly independent solutions of the form (5.26) for (5.17) efficiently. Plugging the ansatz (5.26) into (5.17) and performing coefficient comparison with respect to $\ln^k(z)z^j$ yields (5.25) with $c(j) = c_k(j)$. Using our earlier calculation to determine the initial values, we obtain n_k linearly independent truncated sequences of length r. Reusing the technology for the log-free contribution we can now compute the first $N+1$ coefficients efficiently of the $\ln^k(z)$-contribution in terms of the free coefficients $c_k(0), \ldots, c_k(n_k-1)$. Now define

$$G(z) = \ln^k(z) \sum_{j=0}^{\infty} c_k(j) z^j \tag{5.27}$$

and

$$\tilde{F}(z) = \sum_{i=0}^{k-1} \ln^i(z) \sum_{j=0}^{\infty} c_i(j) z^j, \tag{5.28}$$

i.e., $F(z) = \tilde{F}(z) + G(z)$. Thus replacing $F(z)$ by $\tilde{F}(z) + G(z)$ in (5.17) and moving $G(z)$ (and their derivatives) to the right hand side leads to

$$a_0(z)F(z) + a_1(z)\frac{d}{dz}F(z) + \cdots + a_r(z)\frac{d^r}{dz^r}F(z) = H(z) \tag{5.29}$$

with

$$H(z) = \sum_{i=0}^{k-1} \ln^i(z) \sum_{j=-v}^{\infty} d_i(j) z^j, \tag{5.30}$$

where the $d_i(j) \in \mathbb{Q}$ up to the order N in z are given explicitly. Now we repeat this strategy. By plugging in $\tilde{F}(z)$ into this new differential equation and doing coefficient comparison with respect to $\ln^{k-1}(z)z^j$ yields a linear recurrence of the form

$$b_0(j)c_{k-1}(j) + b_1(j)c_{k-1}(j+1) + \cdots + b_u(j)c_{k-1}(j+u) = d_{k-1}(j+\ell) \tag{5.31}$$

for some integer ℓ. Again we can use the knowledge of the initial values coming from the preprocessing step to prolong the values for $j = r, \ldots, N$ by using the inhomogeneous recurrence. Here we can again apply the tools we used for the log-free case with a slight modification to handle also inhomogeneous contributions. Applying this method iteratively, for $k, k-1, \ldots, 0$ delivers the desired r solutions of (5.26) up to the order N. In this process we remark that the left hand-side of (5.31) remains the same and only the right-hand sides need to be updated. This observation can be utilized to produce only once (5.31) for a symbolic (unevaluated) right-hand side that subsequently can be used to produce the new explicit right-hand sides for $k, k-1, \ldots, 0$.

The above approach for power series expansions (5.24) in z can be extended straightforwardly to Laurent series expansions with $l \in \mathbb{Z}$. As an example, consider the axial-vector function $f^{(-4)}_{a,2\,;3,3}(s)$, corresponding to the color factor $C_3 = C_A^2 C_F$ and the constant $\kappa_3 = \zeta_3$. Its expansion is given by Eq. (5.4)[15]. The corresponding differential equation in z is of order 49, see Table 1. Every coefficient in the expansion can be expressed as a linear combination of the following 49 independent coefficients:

$$\Big\{ b^{(-4)}_{a,2\,;3,3,0,-2}\,,\; b^{(-4)}_{a,2\,;3,3,0,0}\,,\; b^{(-4)}_{a,2\,;3,3,0,1}\,, b^{(-4)}_{a,2\,;3,3,0,2}\,, \ldots, b^{(-4)}_{a,2\,;3,3,0,43}\,,$$

[15] In this particular case, the lower bound of the summation index k is -2, instead of -4. As we explained before, the corresponding coefficients for $k < -2$ are then equal to zero.

$$b^{(-4)}_{a,2\,;\,3,3,1,0}\,,\; b^{(-4)}_{a,2\,;\,3,3,1,1}\,,\; b^{(-4)}_{a,2\,;\,3,3,2,0}\,,\; b^{(-4)}_{a,2\,;\,3,3,2,1}\Big\}\,. \tag{5.32}$$

The following are a few illustrative examples of the relations between the coefficients:

$$\begin{aligned}
b^{(-4)}_{a,2\,;\,3,3,2,2} &= 0.007812500000\, b^{(-4)}_{a,2\,;\,3,3,2,0} - 0.03125000000\, b^{(-4)}_{a,2\,;\,3,3,2,1} && (5.33)\\
b^{(-4)}_{a,2\,;\,3,3,2,3} &= -0.03356933594\, b^{(-4)}_{a,2\,;\,3,3,2,0} - 0.07031250000\, b^{(-4)}_{a,2\,;\,3,3,2,1} && (5.34)\\
b^{(-4)}_{a,2\,;\,3,3,1,2} &= 0.001815795898\, b^{(-4)}_{a,2\,;\,3,3,0,-2} + 0.007812500000\, b^{(-4)}_{a,2\,;\,3,3,1,0}\\
&\quad -0.03125000000\, b^{(-4)}_{a,2\,;\,3,3,1,1} + 4.121093750\, b^{(-4)}_{a,2\,;\,3,3,2,0}\\
&\quad +9.000000000\, b^{(-4)}_{a,2\,;\,3,3,2,1} && (5.35)\\
b^{(-4)}_{a,2\,;\,3,3,1,3} &= 0.001866340637\, b^{(-4)}_{a,2\,;\,3,3,0,-2} - 0.03356933594\, b^{(-4)}_{a,2\,;\,3,3,1,0}\\
&\quad -0.07031250000\, b^{(-4)}_{a,2\,;\,3,3,1,1} + 2.156548394\, b_{a,2\,;\,3,3,2,0}\\
&\quad +4.407118056\, b^{(-4)}_{a,2\,;\,3,3,2,1} && (5.36)\\
b^{(-4)}_{a,2\,;\,3,3,0,44} &= 1.295717677\times 10^{-59}\, b^{(-4)}_{a,2\,;\,3,3,0,-2} - 1.460958567\times 10^{-48}\, b^{(-4)}_{a,2\,;\,3,3,0,2}\\
&\quad +2.564253656\times 10^{-44}\, b^{(-4)}_{a,2\,;\,3,3,0,3} + \ldots + 5.652741729\, b^{(-4)}_{a,2\,;\,3,3,0,43}\\
&\quad -4.777417126\times 10^{-58}\, b^{(-4)}_{a,2\,;\,3,3,1,0} - 8.784518590\times 10^{-58}\, b^{(-4)}_{a,2\,;\,3,3,1,1}\\
&\quad +1.459368840\times 10^{-51}\, b^{(-4)}_{a,2\,;\,3,3,2,0} + 2.847550234\times 10^{-51}\, b^{(-4)}_{a,2\,;\,3,3,2,1}\,. && (5.37)
\end{aligned}$$

The floating point numbers in front of the coefficients were computed with 5000 digits. Here we are showing only 10 of them.

5.3 Determining the free coefficients by matching

The coefficient relations can now be substituted into large truncated versions of the corresponding series expansions, i.e., expansions in which the sums over k in Eqs. (5.1–5.9) are truncated at a sufficiently large value N. In this way, each truncated expansion is expressed solely in terms of its independent coefficients. The expansions can then be evaluated at any point within their respective radii of convergence, allowing consecutive expansions with overlapping regions of convergence to be matched and the independent coefficients to be determined numerically.

To estimate the numerical precision of the coefficients obtained in this way, we introduce an additional coefficient into each expansion corresponding to a term that is known to be absent. For example, the expansion around a regular point s_0 contains only non-negative powers of z. We therefore formally extend the expansion to start at $k = -1$, introducing the coefficient $b^{(s_0)}_{I;j,l,i,-1}$. Since this coefficient is known to vanish identically, any non-zero value obtained from the matching procedure provides a direct estimate of the numerical error. We refer to this quantity as the *test coefficient*.

Suppose that the independent coefficients of one expansion have already been determined numerically. To determine the coefficients of the next expansion, written in terms of its independent coefficients together with the test coefficient, we evaluate both expansions at $r+1$ distinct points in the overlap of their convergence regions[16] and equate the corresponding values. This yields a linear system of $r+1$ equations for the $r+1$ unknown coefficients. A convenient choice of matching points is

$$\xi \in \{s_{\text{ini}} + n\delta;\; n = 0, \ldots, r\}\,, \tag{5.38}$$

[16]The evaluation is performed using the Feynman prescription, according to which s is understood to have an infinitesimal positive imaginary part. This is particularly important for expansions around singular points, where logarithms and square roots are present.

where the initial point s_{ini} and the spacing δ are chosen so that every point in ξ lies within the common region of convergence of the two expansions. The values of δ were chosen in the range from 1/5000 to 1/20000.

The numerical accuracy of the matching depends on the choice of the points ξ. In practice, we scan different values of s_{ini} and δ and select the combination that minimizes the magnitude of the test coefficient, thereby maximizing the precision of the extracted independent coefficients.

Once the independent coefficients have been determined numerically, they can be substituted into the corresponding coefficient relations to obtain all remaining coefficients numerically. This, in turn, allows the corresponding expansion to be evaluated numerically at any value of s within its radius of convergence.

The precision of the coefficients obtained with the matching procedure also depends on the truncation order N. As expected, increasing N generally improves the numerical accuracy, but at the cost of a more demanding computation. The value of N must therefore be chosen large enough to achieve the desired precision, while keeping the computational cost within reasonable limits.

As mentioned previously, the expansion around $s = 0$ was computed up to $N = 100000$ terms. Although such a large truncation order is not strictly necessary, it could be obtained efficiently using the corresponding recurrence relations, requiring only moderate computational resources. Moreover, the resulting highly accurate expansion provides an excellent starting point for the subsequent matching procedure.

For the remaining expansion points, where the coefficients were obtained using the matching method described above, substantially smaller values of N were sufficient. For the weight $\mathsf{w} = 4$ constants listed in (4.2), we used $N = 5000$ for all expansion points with negative values of s in (5.11), while for the positive expansion points in (5.12) we used $N = 10000$, except at $s = 16$, where $N = 5000$ was sufficient. At $s \to \infty$, we used $N = 4000$. These truncation orders were more than adequate to obtain the numerical precision required to reconstruct all coefficients of the asymptotic expansions at $s \to \infty$ by applying the PSLQ algorithm. In practice, considerably smaller values of N would likely have been sufficient. However, since it is difficult to predict in advance the minimum truncation order required for a successful PSLQ reconstruction, we opted for a large value that remained computationally feasible. For the contribution proportional to $\kappa_4 = l_2\zeta_2$, we used $N = 5000$ for all finite expansion points in (5.14) and (5.13), and $N = 3000$ at $s \to \infty$.

The most demanding cases are those corresponding to $\kappa_1 = 1$, $\kappa_2 = \zeta_2$, and $\kappa_3 = \zeta_3$, for which substantially larger truncation orders are required. For the expansion points listed in (5.15), as well as for the expansions at $s \to \infty$, we used $N = 10000$. For $\kappa_1 = 1$ and $s = -1$, $s = -5/4$, $s = -3/4$ we used even $N = 16000$ coefficients. Computing expansions of this length is particularly challenging because of the high order of the differential equations and the large degree of the associated polynomial coefficients, see Tables 1 and 2. Such a large value of N proved essential in the case $\kappa_1 = 1$ to achieve the precision required for the PSLQ reconstruction. For the cases $\kappa_2 = \zeta_2$ and $\kappa_3 = \zeta_3$, somewhat smaller truncation orders, such as $N = 8000$ or even $N = 7000$, would probably have been sufficient. Nevertheless, as in the weight $\mathsf{w} = 4$ case, it was not possible to determine this beforehand, and therefore we preferred to use a larger value to ensure that the numerical precision at $s \to \infty$ was comfortably adequate to use the PSLQ algorithm, see Section 6.

For the positive expansion points listed in (5.16), we used $N = 8000$ for $\kappa_1 = 1$ and $N = 4000$ for both $\kappa_2 = \zeta_2$ and $\kappa_3 = \zeta_3$. Smaller values would probably have sufficed, since, unlike in [13], our objective here is not necessarily to apply the PSLQ algorithm to the coefficients of the expansions around $s = 4$. Nevertheless, we again chose relatively large truncation orders in

order to obtain a comparable level of numerical precision across all expansion points.

6 The high energy limit

We consider the range $s \in [0, -\infty[$. As we explained in Section 5, in order to approach the high energy limit we construct overlapping series moving from $s = 0$ to $s = -\infty$. The (logarithmic modulated) expansions at $s \to \infty$ associated to each constant in Eq. (2.23) and each color factor in Eq. (2.18) are given in Eq. (5.9). We obtain the form factors by combining these expansions using Eq. (5.10), after which the square roots disappear and we are left with integer powers of $-1/s$. The representation of the form factors around $s \to \infty$ is then given by

$$F_I(s) = \sum_{i=1}^{3} C_i \sum_{l=0}^{6} \sum_{k=0}^{\infty} \tilde{c}_{I;i,l,k} \ln^l\left(-\frac{1}{s}\right) \frac{1}{s^k}. \tag{6.1}$$

A central question concerns the functional structure of the coefficients $\tilde{c}_{I;i,l,k}$. In the quarkonic case they were given for each color factor by ζ-values only.

After performing the matchings described in Section 5 we rationalized the coefficients in Eq. (5.9). Our accuracy has been chosen such that we could use integer formalisms like PSLQ [110–112] to determine the corresponding coefficients in analytic form. After summing all the contributions in Eq. (5.10), the coefficients $\tilde{c}_{I;i,l,k}$ turned out to be rational combinations of the following set of constants,

$$\begin{aligned}&\big\{1,\, \zeta_2,\, \zeta_3,\, \zeta_2^2,\, \zeta_5,\, \zeta_2^3,\, \zeta_3^2,\, \zeta_2\zeta_3,\, l_2^4,\, l_2^5,\, l_2\zeta_2,\, l_2\zeta_3,\, l_2\zeta_2^2,\\ &\quad l_2^2\zeta_2,\, l_2^2\zeta_2^2,\, l_2^3\zeta_2,\, l_2^4\zeta_2,\, l_2\zeta_2\zeta_3,\, a_4,\, a_5,\, \zeta_2 a_4,\, s_6\big\}\end{aligned} \tag{6.2}$$

and three further constants $\tilde{\kappa}_1$, $\tilde{\kappa}_2$, $\tilde{\kappa}_3$ contribute. It is worth mentioning that the coefficients of the intermediate expansions given in Eq. (5.9) were complex numbers. The real parts of these numbers also included the constants

$$\left\{l_2\,, l_2^2\,, l_2^3\,, l_2^2\zeta_3,\, \frac{1}{\pi^2},\, \frac{\zeta_3}{\pi^2}\,, \frac{\zeta_5}{\pi^2},\, \frac{\zeta_3^2}{\pi^2},\, \frac{\zeta_3\zeta_5}{\pi^2}\,, \frac{l_2^4}{\pi^2},\, \frac{a_4}{\pi^2},\, \frac{l_2^4\zeta_3}{\pi^2},\, \frac{\zeta_3 a_4}{\pi^2},\, \frac{\tilde{\kappa}_1}{\pi^2},\, \frac{\tilde{\kappa}_2}{\pi^2},\, \frac{\tilde{\kappa}_3}{\pi^2}\right\}, \tag{6.3}$$

while the imaginary parts could be expressed as rational linear combinations of the following constants,

$$\begin{aligned}&\big\{\pi,\, \pi^3,\, \pi^5,\, \pi l_2,\, \pi^3 l_2,\, \pi^5 l_2,\, \pi l_2^2,\, \pi^3 l_2^2,\, \pi l_2^3,\, \pi^3 l_2^3,\, \pi l_2^4,\, \pi l_2^5,\\ &\quad \pi a_4,\, \pi l_2 a_4,\, \pi\zeta_3,\, \pi^3\zeta_3,\, \pi l_2\zeta_3,\, \pi l_2^2\zeta_3\big\}\,.\end{aligned} \tag{6.4}$$

After combining the results in Eq. (5.10), the constants listed in Eq. (6.3) cancel out from the final result. Furthermore, the imaginary contributions, expressed in terms of the constants in Eq. (6.4), cancel exactly, leaving only real coefficients.

The different constants can be represented as iterated integrals,

$$\mathrm{H}_{b,\vec{a}}(1) = \int_0^1 dx f_b(x) \mathrm{H}_{\vec{a}}(x) \tag{6.5}$$

of letters $f_c(x)$ in the alphabet $\mathfrak{A}$,

$$\mathfrak{A} = \left\{f_0(x), f_1(x), f_{-1}(x)\right\} \equiv \left\{\frac{1}{x}, \frac{1}{1-x}, \frac{1}{1+x}\right\}. \tag{6.6}$$

Here

$$l_2 = \mathrm{H}_{-1}(1), \tag{6.7}$$

$$a_4 = -\frac{1}{24}\mathrm{H}_{-1}(1)^4 + \frac{1}{4}\mathrm{H}_{-1}(1)^2\mathrm{H}_{0,1}(1) + \frac{1}{10}\mathrm{H}_{0,1}(1)^2 + \frac{1}{2}\mathrm{H}_{0,0,-1,1}(1), \tag{6.8}$$

$$\begin{aligned} a_5 = {} & \frac{1}{120}\mathrm{H}_{-1}(1)^5 - \frac{1}{12}\mathrm{H}_{-1}(1)^3\mathrm{H}_{0,1}(1) - \frac{19}{80}\mathrm{H}_{-1}(1)\mathrm{H}_{0,1}(1)^2 + \frac{7}{32}\mathrm{H}_{-1}(1)^2\mathrm{H}_{0,0,1}(1) \\ & -\frac{3}{16}\mathrm{H}_{0,1}(1)\mathrm{H}_{0,0,1}(1) + \frac{153}{128}\mathrm{H}_{0,0,0,0,1}(1) + \frac{1}{4}\mathrm{H}_{0,0,-1,-1,1}(1). \end{aligned} \tag{6.9}$$

We first note the occurrence of the constant

$$s_6 = \zeta_6 - \mathrm{H}_{0,0,0,0,-1,1}(1), \quad \zeta_6 = \mathrm{H}_{0,0,0,0,0,1}(1) \tag{6.10}$$

in a final physical expression, with $\mathrm{H}_{\vec{a}}(x)$ harmonic polylogarithms [107].

Since in the color–planar case [8] cyclotomic harmonic polylogarithms [106] of cyclotomy `c = 6` contributed we searched for corresponding constants of this kind [106, 118]. The constants $\tilde{\kappa}_1$ to $\tilde{\kappa}_3$ were found as the following iterative integrals

$$\tilde{\kappa}_1 = \frac{3^5}{2^2}\mathrm{H}_{\{3,0\},0,0}(1) = \pi^3\sqrt{3} = 53.7044465638173512 97, \tag{6.11}$$

$$\tilde{\kappa}_2 = \frac{3^5}{2^4}\mathrm{H}_{\{3,0\},0,0}(1)\left[\frac{3}{2}\mathrm{H}_{\{3,0\},0}(1) - \mathrm{H}_{\{6,0\},0}(1)\right] = \pi^3\mathrm{Cl}_2\left(\frac{\pi}{3}\right) = 31.469560262685681691, \tag{6.12}$$

$$\tilde{\kappa}_3 = \frac{3^5}{2^2}\mathrm{H}_{\{3,0\},0,0}(1)\mathrm{H}_{\{\{4,-2,1\},0\},0,0}(1) = \pi^3\mathsf{Im}\mathrm{Li}_3\left[\frac{1}{2}e^{i\pi/3}\right] = 14.233090050526350538. \tag{6.13}$$

Terms of the kind $\pi^3\sqrt{3}$ are given by

$$\pi^3\sqrt{3} = \frac{3^2}{2^3}\left[\psi^{(2)}\left(\frac{2}{3}\right) - \psi^{(2)}\left(\frac{1}{3}\right)\right], \tag{6.14}$$

with $\psi(x)$ the di-gamma function. Eq. (6.14) can be expressed by the cyclotomic numbers

$$\sum_{k=0}^{\infty}\frac{1}{(lk+m)^n} = \frac{1}{\Gamma(n)}\left(-\frac{1}{l}\right)^n\psi^{n-1}\left(\frac{m}{l}\right), \tag{6.15}$$

related to the Hurwitz ζ-function [119]. The function $\mathrm{Cl}_2(\varphi)$ denotes the Clausen function [63, 64, 120]

$$\mathrm{Cl}_2(\varphi) = \sum_{k=1}^{\infty}\frac{\sin(k\varphi)}{k^2} = -\int_0^{\varphi}\ln\left|2\sin\left(\frac{x}{2}\right)\right|dx. \tag{6.16}$$

The letters forming the iterated integrals in Eqs. (6.10,6.11–6.13) are finally given by those of $\mathfrak{A}$ and

$$f_{\{3,0\}}(x) = \frac{1}{1+x+x^2}, \quad f_{\{6,0\}}(x) = \frac{1}{1-x+x^2}, \tag{6.17}$$

$$f_{\{4,-2,1\},0}(x) = \frac{1}{4-2x+x^2}. \tag{6.18}$$

and are either cyclotomic (6.17) or are numbers related to letters induced by quadratic forms, (6.18), cf. Ref. [121]. The letters (6.6) span the harmonic polylogarithms.

As examples we are showing the asymptotic expansions of the unrenormalized $O(\varepsilon^0)$ contributions of the form factors $F_{V,1}$ and $F_{V,2}$ up to $O(1/s^5)$. Setting $N_c = 3$, and defining $\mathrm{ls} = -\ln(-s)$, they are given by

$$
\begin{aligned}
F_{V,1}^{s\to\infty} &= 64\Bigg\{\left[-\frac{1}{27}+\frac{49}{12960s}-\frac{47}{810s^2}-\frac{259}{1440s^3}-\frac{491}{1944s^4}+\frac{14189}{9720s^5}\right]\mathrm{ls}^6 \\
&+\left[\frac{119}{432}-\frac{407}{480s}-\frac{16051}{12960s^2}-\frac{15751}{3888s^3}-\frac{945889}{77760s^4}-\frac{2023951}{97200s^5}\right]\mathrm{ls}^5 \\
&+\Bigg[\left(-\frac{20}{81}+\frac{3673}{1296s}+\frac{10195}{288s^2}+\frac{197359}{648s^3}+\frac{2660755}{1296s^4}+\frac{7902395}{648s^5}\right)\zeta_2 \\
&-\frac{1681}{864s}-\frac{571873}{10368s^2}-\frac{58338557}{116640s^3}-\frac{2353102207}{680400s^4}-\frac{679446541129}{32659200s^5}+\frac{3143}{1728}\Bigg]\mathrm{ls}^4 \\
&+\Bigg[\left(\frac{977}{648}-\frac{12475}{648s}-\frac{118505}{432s^2}-\frac{1264817}{486s^3}-\frac{349389229}{19440s^4}-\frac{52045981}{486s^5}\right)\zeta_2 \\
&+\left(\frac{110531688486577}{457228800}-\frac{9532379}{162}\zeta_3\right)\frac{1}{s^5}+\left(\frac{23621245300801}{571536000}-\frac{3261179}{324}\zeta_3\right)\frac{1}{s^4} \\
&+\left(\frac{21800859401}{3499200}-\frac{41224}{27}\zeta_3\right)\frac{1}{s^3}+\left(\frac{5819821}{7776}-\frac{120311}{648}\zeta_3\right)\frac{1}{s^2} \\
&+\left(\frac{107167}{1296}-\frac{475}{36}\zeta_3\right)\frac{1}{s}-\frac{254}{81}\zeta_3+\frac{7579}{2592}\Bigg]\mathrm{ls}^3 \\
&+\Bigg[\left(-\frac{97}{54}-\frac{44093}{2160s}-\frac{516317}{2160s^2}-\frac{143461}{72s^3}-\frac{811891}{60s^4}-\frac{89472121}{1080s^5}\right)\zeta_2^2 \\
&+\frac{527}{54}\zeta_3+\left(\frac{2140}{27}\zeta_3+\frac{107609}{324}\right)\frac{1}{s}+\left(\frac{249451}{144}\zeta_3+\frac{40985165}{31104}\right)\frac{1}{s^2}+\left(\frac{9939443}{648}\zeta_3\right. \\
&\left.-\frac{6965769779}{11664000}\right)\frac{1}{s^3}+\left(\frac{225487789}{2160}\zeta_3-\frac{1207505059525747}{30005640000}\right)\frac{1}{s^4}+\left(\frac{805169507}{1296}\zeta_3\right. \\
&\left.-\frac{1045382913180275311}{2880541440000}\right)\frac{1}{s^5}-\frac{605705}{7776}+\left(-\frac{2}{3}l_2-\frac{13537}{216s}+\left(\frac{29}{9}l_2\right.\right. \\
&\left.\left.-\frac{111209}{144}\right)\frac{1}{s^2}+\left(\frac{158}{9}l_2-\frac{138093007}{38880}\right)\frac{1}{s^3}+\left(\frac{2482}{27}l_2-\frac{5152806637}{453600}\right)\frac{1}{s^4}\right. \\
&\left.+\left(\frac{7028}{15}l_2-\frac{18453162643}{1088640}\right)\frac{1}{s^5}-\frac{3979}{288}\right)\zeta_2\Bigg]\mathrm{ls}^2 \\
&+\left[\frac{2}{9}l_2^4+\left(\frac{8573}{1080}+\frac{29899}{120s}+\frac{390703}{144s^2}+\frac{75849491}{3240s^3}+\frac{549568937}{3600s^4}+\frac{28296209321}{32400s^5}\right)\zeta_2^2\right.
\end{aligned}
$$

$$+\frac{16}{3}a_4+\zeta_2\left(\frac{8}{3}l_2^2-\frac{22}{3}l_2+\left(\frac{631208}{405}l_2^2-\frac{1303548121}{25200}l_2\right.\right.$$
$$\left.-\frac{748013}{54}\zeta_3-\frac{2039036264236301}{1143072000}\right)\frac{1}{s^5}+\left(\frac{30848}{81}l_2^2-\frac{326120357}{37800}l_2-\frac{15317}{6}\zeta_3\right.$$
$$\left.-\frac{45991144470073}{142884000}\right)\frac{1}{s^4}+\left(\frac{2432}{27}l_2^2-\frac{688471}{540}l_2-\frac{34783}{108}\zeta_3-\frac{30583655261}{583200}\right)\frac{1}{s^3}$$
$$+\left(\frac{560}{27}l_2^2-\frac{8153}{54}l_2+\frac{121}{432}\zeta_3-\frac{18626471}{2592}\right)\frac{1}{s^2}+\left(-\frac{20}{27}l_2^2-\frac{83}{9}l_2\right.$$
$$\left.-\frac{905}{216}\zeta_3-\frac{307519}{432}\right)\frac{1}{s}-\frac{37}{27}\zeta_3-\frac{27295}{288}\Bigg)+\frac{5113}{36}\zeta_3+\left(\frac{76154}{1215}l_2^4+\frac{609232}{405}a_4\right.$$
$$\left.-\frac{28539584419}{21600}\zeta_3-\frac{17712283}{108}\zeta_5+\frac{50172038578234115621}{18517766400000}\right)\frac{1}{s^5}+\left(\frac{3053}{243}l_2^4\right.$$
$$\left.+\frac{24424}{81}a_4-\frac{127902022793}{680400}\zeta_3-\frac{3435319}{108}\zeta_5+\frac{7652263475838252013}{16803158400000}\right)\frac{1}{s^4}$$
$$+\left(\frac{197}{81}l_2^4+\frac{1576}{27}a_4-\frac{6478301}{324}\zeta_3-\frac{1121707}{216}\zeta_5+\frac{1975638199433}{29160000}\right)\frac{1}{s^3}$$
$$+\left(\frac{67}{162}l_2^4+\frac{268}{27}a_4-\frac{334127}{432}\zeta_3-\frac{520027}{864}\zeta_5+\frac{47577215}{5832}\right)\frac{1}{s^2}$$
$$+\left(\frac{10}{81}l_2^4+\frac{80}{27}a_4-\frac{755}{27}\zeta_3-\frac{9665}{432}\zeta_5+\frac{2940227}{3888}\right)\frac{1}{s}+\frac{8}{9}\zeta_5-\frac{4957}{9}\Bigg]\mathrm{ls}$$
$$-\frac{16}{405}l_2^5-\frac{7705}{1944}l_2^4+\left(\frac{80947}{11340}+\frac{5891705}{81648s}+\frac{33439039}{34020s^2}+\frac{36748981}{4536s^3}+\frac{257579593}{4860s^4}\right.$$
$$\left.+\frac{12552412975}{40824s^5}\right)\zeta_2^3+\left(-\frac{5}{9}l_2^2+\frac{32}{135}l_2+\left(\frac{667}{108}l_2^2-\frac{244}{135}l_2+\frac{6839519}{6480}\right)\frac{1}{s}\right.$$
$$+\left(\frac{6185}{72}l_2^2+\frac{874}{27}l_2+\frac{168588197}{12960}\right)\frac{1}{s^2}+\left(\frac{14519}{18}l_2^2+\frac{7568}{45}l_2\right.$$
$$\left.+\frac{37711528277}{388800}\right)\frac{1}{s^3}+\left(\frac{154076}{27}l_2^2+\frac{116132}{135}l_2+\frac{24875134912819}{40824000}\right)\frac{1}{s^4}$$
$$+\left(\frac{104360}{3}l_2^2+\frac{2853992}{675}l_2+\frac{564913601711447}{163296000}\right)\frac{1}{s^5}+\frac{143363}{1440}\Bigg)\zeta_2^2+\frac{199}{288}\zeta_3^2$$
$$-\frac{7705}{81}a_4+\frac{128}{27}a_5+\frac{144233}{432}\zeta_3+\zeta_2\left(\frac{5}{54}l_2^4+\frac{32}{81}l_2^3-\frac{6235}{162}l_2^2\right.$$
$$+\left(\frac{35}{18}\zeta_3+\frac{6965}{54}\right)l_2+\frac{20}{9}a_4-\frac{19067}{432}\zeta_3+\left(-\frac{667}{648}l_2^4-\frac{64}{81}l_2^3\right.$$

$$-\frac{358}{9}l_2^2+\left(282-\frac{1463}{72}\zeta_3\right)l_2-\frac{667}{27}a_4+\frac{148987}{648}\zeta_3-\frac{90995}{54}\Bigg)\frac{1}{s}$$
$$+\Bigg(-\frac{5801}{432}l_2^4-\frac{160}{81}l_2^3+\frac{340}{9}l_2^2+\left(\frac{176129}{162}-\frac{41503}{144}\zeta_3\right)l_2$$
$$-\frac{5801}{18}a_4+\frac{152855}{54}\zeta_3-\frac{97581929}{7776}\Bigg)\frac{1}{s^2}+\Bigg(-\frac{40037}{324}l_2^4-\frac{256}{9}l_2^3$$
$$+\frac{1419908}{1215}l_2^2+\left(\frac{32044222}{6075}-\frac{99673}{36}\zeta_3\right)l_2-\frac{80074}{27}a_4$$
$$+\frac{32068373}{1296}\zeta_3-\frac{108629217289}{1458000}\Bigg)\frac{1}{s^3}+\Bigg(-\frac{7822}{9}l_2^4-\frac{17408}{81}l_2^3+\frac{395239748}{42525}l_2^2$$
$$+\left(\frac{42591525673}{1488375}-\frac{177982}{9}\zeta_3\right)l_2-\frac{62576}{3}a_4+\frac{3239859149}{19440}\zeta_3$$
$$-\frac{129811254513023}{333396000}\Bigg)\frac{1}{s^4}+\Bigg(-\frac{428180}{81}l_2^4-\frac{108416}{81}l_2^3+\frac{490726262}{8505}l_2^2$$
$$+\left(\frac{14829601479241}{95256000}-\frac{1090390}{9}\zeta_3\right)l_2-\frac{3425440a_4}{27}+\frac{38342426077}{38880}\zeta_3$$
$$-\frac{683253287727603317}{360067680000}\Bigg)\frac{1}{s^5}+\frac{927827}{2592}\Bigg)+\Bigg(\frac{99298}{675}l_2^5-\frac{105124618397}{8164800}l_2^4$$
$$-\frac{4267943}{216}\zeta_3^2-\frac{21441655613}{94478400}\tilde{\kappa}_1-\frac{3247522}{10935}\tilde{\kappa}_2-\frac{82880}{81}\tilde{\kappa}_3-\frac{105124618397}{340200}a_4$$
$$-\frac{794384}{45}a_5-\frac{1302560}{81}s_6+\frac{1708229617067371}{1143072000}\zeta_3-\frac{2195310543401}{233280}\zeta_5$$
$$-\frac{781202250523853512716013}{571643448768000000}\Bigg)\frac{1}{s^5}+\Bigg(\frac{9709}{405}l_2^5-\frac{9482853731}{4082400}l_2^4-\frac{435829}{144}\zeta_3^2$$
$$-\frac{1501427}{34992}\tilde{\kappa}_1-\frac{105527}{2187}\tilde{\kappa}_2-\frac{13280}{81}\tilde{\kappa}_3-\frac{9482853731}{170100}a_4-\frac{77672}{27}a_5-\frac{229760}{81}s_6$$
$$+\frac{52622091553511}{190512000}\zeta_3-\frac{192516053233}{116640}\zeta_5-\frac{113809853554807624541}{705732652800000}\Bigg)\frac{1}{s^4}$$
$$+\Bigg(\frac{49}{15}l_2^5-\frac{22727233}{58320}l_2^4-\frac{266927}{864}\zeta_3^2-\frac{401129}{52488}\tilde{\kappa}_1-\frac{4820}{729}\tilde{\kappa}_2-\frac{22727233}{2430}a_4$$
$$-\frac{1760}{81}\tilde{\kappa}_3-392a_5-\frac{36320}{81}s_6+\frac{2637615317}{58320}\zeta_3-\frac{2012950841}{7776}\zeta_5$$
$$-\frac{32336724212507}{3936600000}\Bigg)\frac{1}{s^3}+\Bigg(\frac{41}{162}l_2^5-\frac{38467}{648}l_2^4+\frac{3473}{1152}\zeta_3^2-\frac{9157}{8748}\tilde{\kappa}_1$$
$$-\frac{143}{243}\tilde{\kappa}_2-\frac{16}{9}\tilde{\kappa}_3-\frac{38467}{27}a_4-\frac{820}{27}a_5-\frac{512}{9}s_6+\frac{5062873}{864}\zeta_3-\frac{10666681}{324}\zeta_5$$
$$+\frac{1161351943}{559872}\Bigg)\frac{1}{s^2}+\Bigg(\frac{32}{405}l_2^5-\frac{893}{108}l_2^4-\frac{683}{64}\zeta_3^2-\frac{13}{243}\tilde{\kappa}_1+\frac{5}{729}\tilde{\kappa}_2$$

$$
\begin{aligned}
&-\frac{1786}{9}a_4-\frac{256}{27}a_5-\frac{80}{27}s_6+\frac{693095}{1296}\zeta_3-\frac{9370877}{3888}\zeta_5+\frac{37778}{81}\Bigg)\frac{1}{s}\\
&-\frac{318019}{864}\zeta_5+\frac{788081}{7776}+O(\mathrm{ls}^6/s^6)\Bigg\},
\end{aligned}
\tag{6.19}
$$

$$
\begin{aligned}
F_{V,2}^{s\to\infty} \;=\; & 64\Bigg\{\left[-\frac{43}{2430s^2}-\frac{1973}{19440s^3}-\frac{521}{810s^4}-\frac{31661}{9720s^5}\right]\mathrm{ls}^6\\
&+\left[\frac{16}{27s}+\frac{529}{360s^2}+\frac{36737}{6480s^3}+\frac{335527}{19440s^4}+\frac{234701}{4860s^5}\right]\mathrm{ls}^5\\
&+\Bigg[\left(\frac{11828169859}{583200}-\frac{1728853}{162}\zeta_2\right)\frac{1}{s^5}+\left(\frac{389591423}{116640}-\frac{31255}{18}\zeta_2\right)\frac{1}{s^4}\\
&+\left(\frac{1231505}{2592}-\frac{77591}{324}\zeta_2\right)\frac{1}{s^3}+\left(\frac{33059}{648}-\frac{1645}{72}\zeta_2\right)\frac{1}{s^2}-\frac{205}{216s}\Bigg]\mathrm{ls}^4\\
&+\Bigg[\left(-\frac{206}{81}\zeta_2-\frac{2683}{72}\right)\frac{1}{s}+\left(149\zeta_2+\frac{8642}{81}\zeta_3-\frac{51019}{108}\right)\frac{1}{s^2}+\Bigg(\frac{23711}{12}\zeta_2\\
&+\frac{10225}{9}\zeta_3-\frac{707251}{144}\Bigg)\frac{1}{s^3}+\left(\frac{7290761}{486}\zeta_2+\frac{223301}{27}\zeta_3-\frac{10250948137}{291600}\right)\frac{1}{s^4}\\
&+\left(\frac{38050922}{405}\zeta_2+\frac{4109758}{81}\zeta_3-\frac{817950539009}{3827250}\right)\frac{1}{s^5}\Bigg]\mathrm{ls}^3\\
&+\Bigg[\left(\frac{6424459}{90}\zeta_2^2+\left(\frac{4865676071}{97200}-\frac{6356}{27}l_2\right)\zeta_2-\frac{437039791}{810}\zeta_3\right.\\
&\left.+\frac{969676241097559}{4286520000}\right)\frac{1}{s^5}+\Bigg(\frac{166663}{15}\zeta_2^2+\left(\frac{55830679}{3240}-40l_2\right)\zeta_2-\frac{13961615}{162}\zeta_3\\
&+\frac{27772594783}{2187000}\Bigg)\frac{1}{s^4}+\left(\frac{81133}{54}\zeta_2^2+\left(\frac{958817}{216}-6l_2\right)\zeta_2-\frac{617723}{54}\zeta_3-\frac{11218685}{2592}\right)\frac{1}{s^3}\\
&+\left(\frac{15853}{108}\zeta_2^2+\left(\frac{22747}{27}-\frac{4}{9}l_2\right)\zeta_2-\frac{25177}{27}\zeta_3-\frac{639259}{324}\right)\frac{1}{s^2}\\
&+\left(\frac{251}{36}\zeta_2+\frac{416}{27}\zeta_3-\frac{1477}{9}\right)\frac{1}{s}\Bigg]\mathrm{ls}^2\\
&+\Bigg[\left(-\frac{4}{81}l_2^4+\frac{7157}{270}\zeta_2^2-\frac{32}{27}a_4+\left(\frac{8}{27}l_2^2+\frac{8}{9}l_2+\frac{51845}{216}\right)\zeta_2\right.\\
&\left.+\frac{2512}{27}\zeta_3-\frac{205843}{648}\right)\frac{1}{s}+\Bigg(-\frac{2}{81}l_2^4-\frac{9492}{5}\zeta_2^2-\frac{16}{27}a_4+\frac{2779}{27}\zeta_3\\
&+\zeta_2\left(\frac{16}{27}l_2^2+\frac{256}{3}l_2+\frac{1811}{54}\zeta_3+\frac{56231}{12}\right)+\frac{51533}{108}\zeta_5-\frac{453752}{81}\Bigg)\frac{1}{s^2}
\end{aligned}
$$

$$+\left(-\frac{7}{81}l_2^4-\frac{5316391}{270}\zeta_2^2-\frac{56}{27}a_4+\frac{271039}{18}\zeta_3+\zeta_2\left(\frac{176}{27}l_2^2+\frac{25358}{27}l_2\right.\right.$$
$$\left.\left.+\frac{11342}{27}\zeta_3+\frac{8905771}{216}\right)+\frac{126890}{27}\zeta_5-\frac{463049833}{7776}\right)\frac{1}{s^3}+\left(-\frac{164}{81}l_2^4-\frac{55476766}{405}\zeta_2^2\right.$$
$$-\frac{1312}{27}a_4+\frac{154072027}{972}\zeta_3+\zeta_2\left(\frac{1408}{27}l_2^2+\frac{2865638}{405}l_2+\frac{172445}{54}\zeta_3\right.$$
$$\left.\left.+\frac{19895774023}{72900}\right)+\frac{3284117}{108}\zeta_5-\frac{3531518369599}{8201250}\right)\frac{1}{s^4}+\left(-\frac{158}{9}l_2^4-\frac{2182382911}{2700}\zeta_2^2\right.$$
$$-\frac{1264}{3}a_4+\frac{28314666569}{24300}\zeta_3+\zeta_2\left(\frac{9200}{27}l_2^2+\frac{3304387}{75}l_2+\frac{938033}{54}\zeta_3\right.$$
$$\left.\left.+\frac{32111077988851}{20412000}\right)+\frac{17634373}{108}\zeta_5-\frac{1588111136598363089}{600112800000}\right)\frac{1}{s^5}\Bigg]\mathrm{ls}$$
$$+\left(-\frac{16}{405}l_2^5+\frac{404}{81}l_2^4+\left(\frac{122}{135}l_2-\frac{124927}{360}\right)\zeta_2^2+\frac{3232}{27}a_4+\frac{128}{27}a_5\right.$$
$$+\zeta_2\left(\frac{32}{81}l_2^3+\frac{992}{27}l_2^2-\frac{1868}{9}l_2-\frac{2305}{54}\zeta_3+\frac{3495}{8}\right)+\frac{35819}{216}\zeta_3+\frac{577}{9}\zeta_5$$
$$\left.-\frac{674143}{648}\right)\frac{1}{s}+\left(-\frac{166}{405}l_2^5+\frac{3152}{81}l_2^4-\frac{30180217}{51030}\zeta_2^3+\left(-\frac{1003}{27}l_2^2-\frac{628}{135}l_2\right.\right.$$
$$\left.\left.-\frac{3800123}{405}\right)\zeta_2^2-\frac{21515}{432}\zeta_3^2+\frac{260}{243}\tilde{\kappa}_1+\frac{232}{729}\tilde{\kappa}_2+\frac{32}{27}\tilde{\kappa}_3+\frac{25216}{27}a_4+\frac{1328}{27}a_5\right.$$
$$+\frac{1024}{27}s_6-\frac{195793}{162}\zeta_3+\zeta_2\left(\frac{907}{162}l_2^4+\frac{320}{81}l_2^3-\frac{856}{27}l_2^2+\left(\frac{2191}{18}\zeta_3\right.\right.$$
$$\left.\left.\left.-\frac{2072}{3}\right)l_2+\frac{3628}{27}a_4-\frac{625295}{324}\zeta_3+\frac{3021521}{324}\right)+\frac{40430395}{1944}\zeta_5-\frac{1480295}{324}\right)\frac{1}{s^2}$$
$$+\left(-\frac{169}{45}l_2^5+\frac{5201}{18}l_2^4-\frac{321994651}{51030}\zeta_2^3+\left(-\frac{16426}{27}l_2^2-\frac{692}{15}l_2\right.\right.$$
$$\left.\left.-\frac{259746577}{3240}\right)\zeta_2^2+\frac{97145}{648}\zeta_3^2+\frac{15031}{2187}\tilde{\kappa}_1+\frac{392}{81}\tilde{\kappa}_2+\frac{4096}{243}\tilde{\kappa}_3+\frac{20804}{3}a_4\right.$$
$$+\frac{1352}{3}a_5+\frac{76672}{243}s_6-\frac{1331983}{54}\zeta_3+\zeta_2\left(\frac{22591}{243}l_2^4+\frac{320}{9}l_2^3\right.$$
$$-\frac{28792}{27}l_2^2+\left(\frac{6307}{3}\zeta_3-\frac{293876}{81}\right)l_2+\frac{180728}{81}a_4-\frac{2156093}{108}\zeta_3$$
$$\left.\left.+\frac{81713761}{1296}\right)+\frac{43715215}{216}\zeta_5-\frac{189711101}{46656}\right)\frac{1}{s^3}+\left(-\frac{2092}{81}l_2^5+\frac{13572359}{7290}l_2^4\right.$$

$$
-\frac{383089676}{8505}\zeta_2^3+\left(-\frac{43879}{9}l_2^2-\frac{8200}{27}l_2-\frac{51806903917}{97200}\right)\zeta_2^2+\frac{1076027}{432}\zeta_3^2
+\frac{562607}{13122}\tilde{\kappa}_1+\frac{9460}{243}\tilde{\kappa}_2+\frac{11200}{81}\tilde{\kappa}_3+\frac{54289436}{1215}a_4+\frac{83680}{27}a_5+\frac{175360}{81}s_6
-\frac{5509262849}{29160}\zeta_3+\zeta_2\left(\frac{120437}{162}l_2^4+\frac{19840}{81}l_2^3-\frac{10613552}{1215}l_2^2+\left(\frac{102011}{6}\zeta_3
-\frac{129789793}{6075}\right)l_2+\frac{481748}{27}a_4-\frac{46607033}{324}\zeta_3+\frac{380815246837}{1093500}\right)
+\frac{100578085}{72}\zeta_5+\frac{64087983862793}{656100000}\Bigg)\frac{1}{s^4}+\Bigg(-\frac{20846}{135}l_2^5+\frac{793387189}{72900}l_2^4
-\frac{2309825303}{8505}\zeta_2^3+\left(-\frac{830825}{27}l_2^2-\frac{235204}{135}l_2-\frac{4553200031557}{1458000}\right)\zeta_2^2
+\frac{7798951}{432}\zeta_3^2+\frac{1319033}{6561}\tilde{\kappa}_1+\frac{184720}{729}\tilde{\kappa}_2+\frac{24320}{27}\tilde{\kappa}_3+\frac{1586774378}{6075}a_4
+\frac{166768}{9}a_5+\frac{116480}{9}s_6-\frac{107122694929}{94500}\zeta_3+\zeta_2\left(\frac{757865}{162}l_2^4
+\frac{118720}{81}l_2^3-\frac{334037996}{6075}l_2^2+\left(\frac{1938965}{18}\zeta_3-\frac{8773381222}{70875}\right)l_2
+\frac{3031460}{27}a_4-\frac{714704789}{810}\zeta_3+\frac{3003044947049837}{1714608000}\right)+\frac{40345127863}{4860}\zeta_5
+\frac{79286374540590832453}{75614212800000}\Bigg)\frac{1}{s^5}+O(\mathrm{ls}^6/s^6)\Bigg\}. \tag{6.20}
$$

The corresponding expressions for $s \to +\infty$ are obtained by setting

$$
\ln(-s) \to \ln(s) + i\pi \tag{6.21}
$$

in the expressions for $s \to -\infty$.

We have tried to guess the polynomial parts in Eq. (6.1) for all form factor expansions up to $O(1/s^{1400})$ as closed functions of s. This has been possible for the most simple contributions. The respective terms yield the representation of the form factor within the convergence radius of the series in closed form. Due to the presence of a threshold at $s = 4$ one expects square-root valued functions. First one obtains infinite sum representations, containing central binomials $\binom{2n}{n}$. These can be handled by algorithms of Ref. [89] and Ref. [122]. Some of these sum-types have also been considered in the earlier literature [123, 124]. A simple example is

$$
\sum_{n=0}^{\infty}\frac{(-27+101n-94n^2-371n^3+754n^4-644n^5+216n^6)}{12(2n-3)(2n-1)^2(1+2n)}\binom{2n}{n}\left(-\frac{1}{s}\right)^n
= \frac{5s^4-36s^3+146s^2-68s+256}{6(s-4)^{5/2}s^{3/2}}+\frac{(s-16)\arcsin\left(\frac{2}{\sqrt{s}}\right)}{24\sqrt{s}}. \tag{6.22}
$$

containing the threshold $\sqrt{s-4}$ and the pseudo-threshold factor $(s-16)$. In the high energy result, logarithms $\ln(\sqrt{4-s})$, cf. Section 7, have been expanded already. This expression signals that the expansion around $s \to \infty$ will diverge at $s = 4$, which is confirmed by applying Cauchy's criterion on the summand in the l.h.s. of Eq. (6.22).

From about 1400 coefficients one can obtain both recurrences and differential equations describing the respective color-ζ values and powers in $\ln(-1/s)$. For the recurrences only a few are first order factorizing and one finds closed form solutions like (6.22).

Here it is convenient to use the variable x instead of s. In the sum-expressions also cyclotomic harmonic sums [106]

$$S_{\{a,b,c\}}(n) = \sum_{k=1}^{N} \frac{1}{(ak+b)^c}, \quad a,b \in \mathbb{Z}\backslash\{0\}, \quad c \in \mathbb{N} \tag{6.23}$$

occur. By using the command `ComputeGeneratingFunction` of `HarmonicSums` [87–90], the result is obtained by finding the corresponding differential equation of the problem. To keep the degrees of the differential equations low, larger polynomials in n should be partial fractioned. The differential equations are then solved in iterating integrals over the letters of the corresponding alphabet, which contains Kummer-Poincaré [125–133]

$$\frac{1}{x-c}, \quad c \in \mathbb{C}, \tag{6.24}$$

and square-root valued letters

$$\sqrt{x}\sqrt{a+x}, \quad \text{etc.} \tag{6.25}$$

We consider one example of the high multiple zeta value $C_F^3\zeta_2 l_2^2$ls. The corresponding recurrence is expected to be still relatively simple. One obtains

$$\sum_{n=0}^{\infty}\left(-\frac{1}{s}\right)^n \left[\frac{(-1)^n\left(27-135n+266n^2-266n^3+176n^4-56n^5\right)\binom{2n}{n}}{6(2n-3)(2n-1)^2}\right.$$
$$\left.+\frac{(-1)^n n\binom{2n}{n}S_{\{2,-1,1\}}(n)}{3(2n-1)}\right] = -\frac{P_1}{6(1-x)^3(1+x)^5}+\frac{2x\ln\left(\frac{1+x}{1-x}\right)}{3(1-x^2)}, \tag{6.26}$$

$$P_1 = 9-2x+88x^2-238x^3+670x^4-238x^5+88x^6-2x^7+9x^8. \tag{6.27}$$

Here the solution depends only on the harmonic polylogarithms $\mathrm{H}_1(x)$ and $\mathrm{H}_{-1}(x)$, after rewriting the Kummer-Poincaré integrals with a more complicated main variable accordingly. The iterated integrals with root-valued letters only occur in intermediate steps of the calculation.

Let us guess the corresponding difference equations and investigate their factorization, cf. Ref. [134]. We consider the case of the C_F^3 term at $O(\varepsilon^0)$ of the form factor $F_{V,1}(s)$. The available number of coefficients allowed to obtain 28 recurrences, out of which 10 are first order factorizing, as illustrated in Table 3.

For the solvable part around $s \to \infty$ of the C_F^3-term for the vector form factor $F_{V,1}(s)$ one obtains

$$F_{V,1}^{s\to\infty,solv.} = 64\left\{\frac{C_F^3}{(1-x)^3(x+1)^5}\right.$$

recurrence				
ls^k	constant	degree	order	# 1st ord.
ls^6	1	18	5	2
ls^4	ζ_2	18	5	2
ls^3	ζ_3	18	5	2
ls^2	ζ_2^2	18	5	2
ls^2	$\ln(2)\zeta_2$	8	2	2
ls	$\mathrm{Li}_4(1/2)$	8	2	2
ls	ζ_5	18	5	2
ls	$\zeta_2\zeta_3$	18	5	2
ls	$\ln^2(2)\zeta_2$	7	2	2
ls	$\ln(2)\zeta_2$	126	19	9
ls	$\ln^4(2)$	8	2	2
1	$\ln^4(2)$	153	22	9
1	$\mathrm{Li}_4(1/2)$	153	22	9
1	$\ln^3(2)\zeta_2$	5	1	1
1	$\ln(2)\zeta_2^2$	8	2	2
1	$\ln^5(2)$	8	2	2
1	$\mathrm{Li}_5(1/2)$	8	2	2
1	ζ_2^3	18	5	2
1	$\ln(2)\zeta_2\zeta_3$	18	5	2
1	$\ln^2(2)\zeta_2^2$	18	5	2
1	$\ln^4(2)\zeta_2$	18	5	2
1	ζ_3^2	18	5	2
1	$\zeta_2\mathrm{Li}_4(1/2)$	18	5	2
1	s_6	3	1	1
1	$\sqrt{3}\pi\zeta_2$	186	20	9
1	$\pi\zeta_2\mathsf{Im}[\mathrm{Li}_2(e^{i\pi/3}]$	41	11	7
1	$\ln^2(2)\zeta_2$	60	12	5
1	$\pi\zeta_2\mathsf{Im}[\mathrm{Li}_3(1+i\sqrt{3})/4]$	1	1	1

Table 3: The parameters of the guessed recurrences for $s \to \infty$ of the C_F^3 term of the form factor $F_{V,1}(s)$.

$$
\begin{aligned}
&\Bigg\{\pi^2 l_2 \mathrm{ls}^2\left[\frac{1}{8}\left(3x^8+3x^7-26x^6-43x^5-130x^4-43x^3-26x^2+3x+3\right)\right.\\
&\left.-\frac{1}{16}\ln\left[\frac{1-x}{1+x}\right](1-x)^2(x+1)^2\left(3x^4+28x^3+22x^2+28x+3\right)\right]\\
&+\mathrm{ls}\left[\frac{1}{48}\ln\left[\frac{1-x}{1+x}\right]l_2^4(1-x)^2(x+1)^2\left(9x^4+68x^3+34x^2+68x+9\right)\right.\\
&+a_4\left(\frac{1}{2}\ln\left[\frac{1-x}{1+x}\right](1-x)^2(x+1)^2\left(9x^4+68x^3+34x^2+68x+9\right)\right.\\
&\left.\left.-18x^8-107x^7+250x^6-925x^5+3136x^4-925x^3+250x^2-107x-18\right)\right.
\end{aligned}
$$

$$
\begin{aligned}
&+\pi^2 l_2^2\Bigg(\frac{1}{6}\left(-9x^8+2x^7-88x^6+238x^5-670x^4+238x^3-88x^2+2x-9\right)\\
&-\frac{2}{3}\ln\left[\frac{1-x}{1+x}\right](1-x)^2x(x+1)^4\Bigg)\\
&-\frac{1}{24}l_2^4\left(18x^8+107x^7-250x^6+925x^5-3136x^4+925x^3-250x^2+107x+18\right)\Bigg]\\
&+\frac{32}{3}\pi^3(1-x)^2x^3\mathsf{Im}\left[\mathrm{Li}_3\left(\frac{1}{4}\left(1+i\sqrt{3}\right)\right)\right]\\
&+a_5\Bigg[\frac{3}{2}\ln\left[\frac{1-x}{1+x}\right](1-x)^2(x+1)^2\left(3x^4+12x^3-10x^2+12x+3\right)\\
&-16x^8+233x^7-1006x^6+3791x^5-8052x^4+3791x^3-1006x^2+233x-16\Bigg]\\
&+l_2^5\Bigg[\frac{1}{120}\left(16x^8-233x^7+1006x^6-3791x^5+8052x^4-3791x^3+1006x^2-233x+16\right)\\
&-\frac{1}{80}\ln\left[\frac{1-x}{1+x}\right](1-x)^2(x+1)^2\left(3x^4+12x^3-10x^2+12x+3\right)\Bigg]\\
&+\pi^4 l_2\Bigg[\frac{1}{180}\left(-4x^8+227x^7-724x^6+1469x^5-8688x^4+1469x^3-724x^2+227x-4\right)\\
&-\frac{1}{120}\ln\left[\frac{1-x}{1+x}\right](1-x)^2(x+1)^2\left(x^2+16x+1\right)\left(3x^2+4x+3\right)\Bigg]\\
&+\frac{8}{3}s_6(1-x)^2\left(3x^4-54x^3+70x^2-54x+3\right)x\\
&-\frac{2}{9}\pi^2 l_2^3\left(x^8-14x^7+64x^6-242x^5+510x^4-242x^3+64x^2-14x+1\right)\Bigg\}\Bigg\},
\end{aligned}
\tag{6.28}
$$

serving as an illustration. Here one has $\mathrm{ls} = -2\ln(1-x)+\ln(x)$, after transforming back to the variable x by which square-root valued iterated integrals are turned into harmonic polylogarithms. The results for the other color factors and currents are similar. The ones for the vector current are given in the ancillary files in complete form.

7 Numerical results for threshold and pseudo-threshold

As we explained in Section 5, the kinematic region $s \in [0,\infty[$ has also been mapped out by overlapping series expansions. Here we used the values listed in (5.12), (5.14) or (5.16) depending on the constant in Eq. (2.23) under consideration.

The values at $s \to +\infty$ are obtained by applying the replacement Eq. (6.21) to Eq. (6.1). The values $s = 4$ and $s = 16$ mark the two-particle threshold and the four-particle pseudo-threshold.

For the two vector currents the most singular terms are[17]

$$F_{V,1}^{s=4} \propto \left[\frac{C_F^3}{(4-s)^{5/2}} + \frac{C_A C_F^2}{(4-s)^{3/2}} + \frac{C_F C_A^2}{\sqrt{4-s}}\right] \ln^3(\sqrt{4-s}), \tag{7.1}$$

$$F_{V,2}^{s=4} \propto \left[\left(\frac{C_F^3}{(4-s)^{5/2}} + \frac{C_A C_F^2}{(4-s)^{3/2}}\right) \ln(\sqrt{4-s}) + \frac{C_F C_A^2}{\sqrt{4-s}}\right] \ln^2(\sqrt{4-s}). \tag{7.2}$$

For all form factors, the highest logarithmic power at threshold is $\ln^3(\sqrt{4-s})$. We set $z = \text{sign}(4-s)\sqrt{4-s}$ and calculate the form factors for QCD ($N_c = 3$),

$$\begin{aligned}
&F_{V,1}^{s=4}(s) = \\
&64\Bigg\{\Bigg[\frac{67.020643276582255754}{z^5} + \frac{196.14487321500817679}{z^3} - \frac{170.34206114472744875}{z^2} \\
&+\frac{240.25908053757386093}{z} + 113.94722282821479673 - 27.034756712385753673z \\
&+9.9213893624530990807z^2 - 47.821614988072272099z^3\Bigg] \ln^3(z) \\
&+\Bigg[-\frac{335.10321638291127877}{z^5} - \frac{140.36770703771532258}{z^4} - \frac{859.35492161827618220}{z^3} \\
&+\frac{527.84106500640866095}{z^2} - \frac{708.69657264031675763}{z} - 230.81098800267870479 \\
&+573.08459738167342666z - 66.333837596732951750z^2 \\
&+246.09111998237592795z^3\Bigg] \ln^2(z) + \Bigg[\frac{1206.4946345102209621}{z^5} \\
&+\frac{935.78471358476881719}{z^4} + \frac{3893.6868101680108198}{z^3} - \frac{2704.8274033004820109}{z^2} \\
&+\frac{2196.4468782816843489}{z} + 419.33347768644876125 - 2738.2988837485641725z \\
&+182.05054208017950358z^2 - 771.12031243138006769z^3\Bigg] \ln(z) \\
&-\frac{1421.8495670486650925}{z^5} - \frac{1681.6788169229116386}{z^4} \\
&-\frac{5201.6536874048176874}{z^3} + \frac{3121.3715770767315534}{z^2} - \frac{260.96293808394154879}{z} \\
&-3411.6235285341735782 + 3671.20423881351756512 \\
&-938.55790702760894830z^2 + 772.18066397138656325z^3 + O(\ln^3(z)z^4)\Bigg\},
\end{aligned} \tag{7.3}$$

$$\begin{aligned}
&F_{V,2}^{s=4}(s) = \\
&64\Bigg\{\Bigg[-\frac{67.020643276582255754}{z^5} + \frac{93.578471358476881719}{z^4} - \frac{146.60765716752368446}{z^3} \\
&-\frac{70.183853518857661289}{z^2} + \frac{8.0672996536626789333}{z} + 5.8486544599048051075
\end{aligned}$$

[17] Eqs. (7.1–7.2) should be interpreted with each color factor having a different constant of proportionality.

$$+17.499107412808146921z + 1.4621636149762012769z^2 + 4.4451765612620808251z^3\Bigg] \ln^3(z)$$

$$+\Bigg[\frac{234.57225146803789514}{z^5} - \frac{233.94617839619220430}{z^4} + \frac{1267.0638348841515714}{z^3}$$

$$-\frac{194.83330169557882014}{z^2} + \frac{343.26860551225689033}{z} + 215.22439177610109378$$

$$+86.629039642351514841z + 51.361586667011192180z^2 + 13.310190423572710157z^3\Bigg] \ln^2(z)$$

$$+\Bigg[-\frac{770.86045321243629969}{z^5} - \frac{81.752298987167572850}{z^4} - \frac{4252.8858245363383188}{z^3}$$

$$+\frac{812.50078143439908563}{z^2} - \frac{668.55658351210289137}{z} - 671.91897951899863342$$

$$-235.76866949907519536z - 136.758188429488017712z^2 + 4.8315736060575201094z^3\Bigg] \ln(z)$$

$$+\frac{651.05064160209897205}{z^5} + \frac{688.55371120890422021}{z^4} + \frac{6515.4518611427798796}{z^3}$$

$$-\frac{1539.4430480039000202}{z^2} + \frac{1443.8094142399721744}{z} - 185.89212672255244637$$

$$+315.58943821132890552z + 137.97759955857833395z^2 - 61.012626525594663345z^3$$

$$+O(\ln^3(z)z^4)\Bigg\}. \tag{7.4}$$

For the representation around $s = 16$ we obtain for the unrenormalized vector form factors $F_{V,1}$ and $F_{V,2}$

$$\begin{aligned} F_{V,1}^{s=16}(s) &= 64\Bigg\{ (2325.4946308219634279 - 487.43159998661110240\ i) \\ &\quad +(22.480629736147760202 + 21.299424286130607709\ i)\ [s-16] \\ &\quad -(0.8743653418526481576 + 1.8387376395950035924\ i)\ [s-16]^2 \\ &\quad +(0.12341341541186443744 + 0.15565964113939265584\ i)\ [s-16]^3 \\ &\quad -(0.013592443881038082748 + 0.011969209955373434833\ i)\ [s-16]^4 \\ &\quad -2.1838658955132801214947 \times 10^{-7}\ i\ [s-16]^{9/2} + O([s-16]^5)\Bigg\}, \end{aligned} \tag{7.5}$$

$$\begin{aligned} F_{V,2}^{s=16}(s) &= 64\Bigg\{-(212.54368142723435665 - 99.697189178112869250\ i) \\ &\quad +(8.529885254529849981 - 16.141024662980248233\ i)\ [s-16] \\ &\quad +(0.1468751565593577835 + 1.4776029465283092534\ i)\ [s-16]^2 \\ &\quad -(0.072252433798853051314 + 0.11790695562822033430\ 7\ i)\ [s-16]^3 \\ &\quad +(0.010259247566952065117 1 + 0.008885041352202496802 3\ i)\ [s-16]^4 \\ &\quad +1.1214446490473600623891 9 \times 10^{-7}\ i\ [s-16]^{9/2} + O([s-16]^5)\Bigg\}. \end{aligned} \tag{7.6}$$

At $s = 4$ we calculated 4000 coefficients per logarithmic power with 1200 digits of precision and, similarly, at $s = 16$, we obtained 4000 coefficients with 300 digits of precision. Notice that in Eqs. (7.5) and (7.6) the lowest non-integer power is $[s-16]^{9/2}$ in both cases. As we mentioned in Section 5, the expansions around $s = 16$ were obtained by matching them directly with the asymptotic expansions at $s \to \infty$.

We have also performed a numerical comparison of our unrenormalized form factors with those of the numerical programme of Ref. [14, 16, 135, 136] at selected values of

$$s \in \left\{ -\frac{1}{10}, -5, -10, -50, -200, 200, 16, 5, 3, 2, 1, \frac{1}{10} \right\} \tag{7.7}$$

spanning a wide range of the kinematic region. We found relative agreement of better than 10^{-10}.

8 Conclusions

We have calculated the gluonic contributions to the massive form factors in the vector, axial-vector, scalar and pseudoscalar cases, adding on the quarkonic contributions [13] computed by us previously. These are all non-singlet contributions. We have performed these calculations as widely as possible analytically. The computer-algebraic efforts to perform the present calculation were extremely large, starting with the integration-by-parts reduction, the calculation of deep analytic expansions in the low energy limit by using the method of arbitrary high moments [61], and the guessing of the necessary difference and differential equations. The matching between the different points in s maintaining very high accuracy constitutes a further challenge, to cover the complete kinematic region analytically in terms of very deep expansions. The guessing of the initial difference and differential equations at $s = 0$ required massive parallelization in the most complicated cases and the use of large mainframes such as the super-computer `MACH-2`. The differential and difference equations obtained in this way belong to the most voluminous ones having been computed so far.

The present calculation has been possible by using very deep Frobenius-expansions of the contributing differential equations, which are used mapping out the whole kinematic region at high numerical accuracy. Starting from $s = 0$ we reached in this way an analytic expansion around $s \to \infty$ for the first time and determined all contributing constants by using integer algorithms. Contrary to the quarkonic case, also non multiple zeta values contribute, which finally are found to belong to the class of iterated integrals described by some of us in Refs. [106, 121]. The s-dependence of some of the contributions could even be determined in closed form in terms of iterated integrals.

We have performed detailed comparisons with the numerical results presented in Refs. [14, 16, 135, 136] before and found relative agreement of better than $O(10^{-10})$. In ancillary files to this paper we present computer-readable analytic results. Numerical codes are also available.

A Codes

The following `Mathematica` codes are provided for the gluonic contributions to the form factors in form of ancillary files. The notebook `EvaluateNumerical.nb` evaluates the unrenormalized $O((\alpha_s/\pi)^3)$ part of the formfactors to $O(10^{-30})$ accuracy in the whole kinematic range of s. The file system is contained in `t1.tar.gz`. Here the analytic pieces of the type (4.8, 4.9)

are not included. They are given as `.m` files in the file `t0.tar.gz`. The guessed color-zeta factors as functions, cf. (6.28), for the cases V1 and V2 for all color factors are given in the file `t2.tar.gz`. The numerical representations of the six unrenormalized and renormalized gluonic form factors to $O(a_s^3)$ are available by the code `FFNUM2.f`. It is available on request via e-mail from `Johannes.Bluemlein@desy.de`.

Acknowledgment. We thank DI J. Messner from Zentraler Informationsdienst (ZID) Johannes Kepler University, Linz, for installing the parallelized guessing software [68] at the supercomputer `MACH-2` of JKU Linz and his help in maintaining the runs determining the largest differential and difference operators in this project. We thank M. Kauers and K. Schönwald for discussions, and D. Broadhurst for his interest in our work. This research was funded in whole or in part by the Austrian Science Fund (FWF) grants DOI 10.55776/P33530, DOI 10.55776/PAT1332123, and DOI 10.55776/I6130.

References

[1] J. Blümlein and C. Schneider, *Analytic computing methods for precision calculations in quantum field theory*, Int. J. Mod. Phys. A **33** (2018) no.17, 1830015 [arXiv:1809.02889 [hep-ph]].

[2] J. Gluza, A. Mitov, S. Moch, and T. Riemann, *The QCD form factor of heavy quarks at NNLO*, JHEP **07** (2009) 001 [arXiv:0905.1137 [hep-ph]].

[3] J.M. Henn, A.V. Smirnov, and V.A. Smirnov, *Analytic results for planar three-loop integrals for massive form factors, JHEP* **12** (2016) 144 [arXiv:1611.06523 [hep-ph]].

[4] J. Henn, A.V. Smirnov, V.A. Smirnov and M. Steinhauser, *Massive three-loop form factor in the planar limit*, JHEP **1701** (2017) 074 [arXiv:1611.07535 [hep-ph]].

[5] T. Ahmed, J.M. Henn and M. Steinhauser, *High energy behaviour of form factors*, JHEP **06** (2017) 125 [arXiv:1704.07846 [hep-ph]].

[6] J. Ablinger, A. Behring, J. Blümlein, G. Falcioni, A. De Freitas, P. Marquard, N. Rana and C. Schneider, *Heavy quark form factors at two loops*, Phys. Rev. D **97** (2018) no.9, 094022 [arXiv:1712.09889 [hep-ph]].

[7] J. Ablinger, J. Blümlein, P. Marquard, N. Rana and C. Schneider, *Heavy Quark Form Factors at Three Loops in the Planar Limit* Phys. Lett. B **782** (2018) 528–532 [arXiv:1804.07313 [hep-ph]].

[8] J. Ablinger, J. Blümlein, P. Marquard, N. Rana and C. Schneider, *Automated Solution of First Order Factorizable Systems of Differential Equations in One Variable*, Nucl. Phys. B **939** (2019) 253–291. [arXiv:1810.12261 [hep-ph]].

[9] R.N. Lee, A.V. Smirnov, V.A. Smirnov and M. Steinhauser, *Three-loop massive form factors: complete light-fermion corrections for the vector current*, JHEP **03** (2018) 136 [arXiv:1801.08151 [hep-ph]].

[10] R.N. Lee, A.V. Smirnov, V.A. Smirnov and M. Steinhauser, *Three-loop massive form factors: complete light-fermion and large-N_c corrections for vector, axial-vector, scalar and pseudo-scalar currents*, JHEP **05** (2018) 187 [arXiv:1804.07310 [hep-ph]].

[11] J. Blümlein, P. Marquard and N. Rana, *Asymptotic behavior of the heavy quark form factors at higher order* Phys. Rev. D **99** (2019) no.1, 016013 [arXiv:1810.08943 [hep-ph]].

[12] J. Blümlein, P. Marquard, N. Rana and C. Schneider, *The Heavy Fermion Contributions to the Massive Three Loop Form Factors*, Nucl. Phys. B **949** (2019) 114751 [arXiv:1908.00357 [hep-ph]].

[13] J. Blümlein, A. De Freitas, P. Marquard, N. Rana and C. Schneider, *Analytic results on the massive three-loop form factors: Quarkonic contributions*, Phys. Rev. D **108** (2023) no.9, 094003 [arXiv:2307.02983 [hep-ph]].

[14] M. Fael, F. Lange, K. Schönwald and M. Steinhauser, *Singlet and nonsinglet three-loop massive form factors*, Phys. Rev. D **106** (2022) 034029 [arXiv:2207.00027 [hep-ph]].

[15] M. Egner, M. Fael, F. Lange, K. Schönwald and M. Steinhauser, *Three-loop nonsinglet matching coefficients for heavy quark currents*, Phys. Rev. D **105** (2022) no.11, 114007 [arXiv:2203.11231 [hep-ph]].

[16] M. Fael, F. Lange, K. Schönwald and M. Steinhauser, *Massive Vector Form Factors to Three Loops*, Phys. Rev. Lett. **128** (2022) 172003 [arXiv:2202.05276 [hep-ph]].

[17] K. Schönwald, *Massive form factors at $\mathcal{O}(\alpha_s^3)$*, PoS (LL2022) 006 [arXiv:2207.06705 [hep-ph]].

[18] M. Fael, F. Lange, K. Schönwald and M. Steinhauser, *Massive three-loop form factors: Anomaly contribution*, Phys. Rev. D **107** (2023) no.9, 094017 [arXiv:2302.00693 [hep-ph]].

[19] K. Schönwald, *Singlet and anomaly contributions to massive QCD form factors* PoS (RADCOR2023) 045.

[20] O.V. Tarasov, A.A. Vladimirov and A.Y. Zharkov, *The Gell-Mann-Low Function of QCD in the Three Loop Approximation*, Phys. Lett. B **93** (1980) 429–432.

[21] S.A. Larin and J.A.M. Vermaseren, *The Three loop QCD Beta function and anomalous dimensions*, Phys. Lett. B **303** (1993) 334–336 [hep-ph/9302208].

[22] T. van Ritbergen, J.A.M. Vermaseren and S.A. Larin, *The Four loop beta function in quantum chromodynamics* Phys. Lett. B **400** (1997) 379–384 [hep-ph/9701390].

[23] M. Czakon, *The Four-loop QCD beta-function and anomalous dimensions*, Nucl. Phys. B **710** (2005) 485–498 [hep-ph/0411261].

[24] K.G. Chetyrkin, *Four-loop renormalization of QCD: Full set of renormalization constants and anomalous dimensions*, Nucl. Phys. B **710** (2005) 499–510 [hep-ph/0405193].

[25] P.A. Baikov, K.G. Chetyrkin and J.H. Kühn, *Five-Loop Running of the QCD coupling constant*, Phys. Rev. Lett. **118** (2017) no.8, 082002 [arXiv:1606.08659 [hep-ph]].

[26] F. Herzog, B. Ruijl, T. Ueda, J.A.M. Vermaseren and A. Vogt, *The five-loop beta function of Yang-Mills theory with fermions*, JHEP **02** (2017) 090 [arXiv:1701.01404 [hep-ph]].

[27] K.G. Chetyrkin, G. Falcioni, F. Herzog and J. A. M. Vermaseren, *Five-loop renormalisation of QCD in covariant gauges*, JHEP **10** (2017) 179 [arXiv:1709.08541 [hep-ph]].

[28] T. Luthe, A. Maier, P. Marquard and Y. Schröder, *The five-loop Beta function for a general gauge group and anomalous dimensions beyond Feynman gauge* JHEP **10** (2017) 166 [arXiv:1709.07718 [hep-ph]].

[29] F.G. Frobenius. *Ueber die Integration der linearen Differentialgleichungen durch Reihen*, J. reine angew. Math. (Crelle) **76** (1873) 214–235.

[30] R. Courant and D. Hilbert, Methods of mathematical physics, I and II, (Springer, Berlin 1024; Interscience Publishers, New York, 1853, 1962).

[31] J. van der Hoeven, *Fast evaluation of holonomic functions near and in singularities*, J. Symbol. Comput. **31** (2001) 717–743.

[32] M. Mezzarobba, *Rigorous multiple-precision evaluation of D-finite functions in Sagemath*, 5th International Congress on Mathematical Software (ICMS 2016), Berlin, Germany (2016), arXiv:1607.01967v1 [cs.SC].

[33] J. Grigo, J. Hoff, P. Marquard and M. Steinhauser, *Moments of heavy quark correlators with two masses: exact mass dependence to three loops*, Nucl. Phys. B **864** (2012) 580–596 [arXiv:1206.3418 [hep-ph]].

[34] S.A. Abramov, D. Khmelnov, A. Ryabenko, *On truncated series involved in exponential- logarithmic solutions of truncated LODEs*, In: Computer Algebra in Scientific Computing, CASC 2022, pp. 18–28, 2022.

[35] P. Nogueira, *Automatic Feynman graph generation*, J. Comput. Phys. **105** (1993) 279–289.

[36] J.A.M. Vermaseren, *New features of FORM*, math-ph/0010025.

[37] M. Tentyukov and J.A.M. Vermaseren, *The Multithreaded version of FORM*, Comput. Phys. Commun. **181** (2010) 1419–1427 [hep-ph/0702279].

[38] T. van Ritbergen, A. N. Schellekens and J. A. M. Vermaseren, *Group theory factors for Feynman diagrams*, Int. J. Mod. Phys. A **14** (1999), 41-96 [hep-ph/9802376].

[39] Y. Schröder and M. Steinhauser, *Four-loop decoupling relations for the strong coupling*, JHEP **01** (2006) 051 [arXiv:hep-ph/0512058 [hep-ph]].

[40] K.G. Chetyrkin, J.H. Kühn and C. Sturm, *QCD decoupling at four loops*, Nucl. Phys. B **744** (2006) 121–135 [arXiv:hep-ph/0512060 [hep-ph]].

[41] K.G. Chetyrkin and M. Steinhauser, *Short distance mass of a heavy quark at order α_s^3*, Phys. Rev. Lett. **83** (1999) 4001–4004 [arXiv:hep-ph/9907509 [hep-ph]].

[42] K.G. Chetyrkin and M. Steinhauser, *The Relation between the MS-bar and the on-shell quark mass at order α_s^3*, Nucl. Phys. B **573** (2000) 617–651 [arXiv:hep-ph/9911434 [hep-ph]].

[43] K. Melnikov and T. v. Ritbergen, *The Three loop relation between the MS-bar and the pole quark masses*, Phys. Lett. B **482** (2000) 99–108 [arXiv:hep-ph/9912391 [hep-ph]].

[44] D.J. Broadhurst, N. Gray and K. Schilcher, *Gauge invariant on-shell Z(2) in QED, QCD and the effective field theory of a static quark*, Z. Phys. C **52** (1991) 111–122.

[45] P. Marquard, A.V. Smirnov, V.A. Smirnov and M. Steinhauser, *Four-loop wave function renormalization in QCD and QED*, Phys. Rev. D **97** (2018) no.5, 054032 [arXiv:1801.08292 [hep-ph]].

[46] P. Marquard, A.V. Smirnov, V.A. Smirnov, M. Steinhauser and D. Wellmann, *$\overline{\text{MS}}$-on-shell quark mass relation up to four loops in QCD and a general $SU(N)$ gauge group*, Phys. Rev. D **94** (2016) no.7, 074025 [arXiv:1606.06754 [hep-ph]].

[47] P. Marquard, A.V. Smirnov, V.A. Smirnov and M. Steinhauser, *Quark Mass Relations to Four-Loop Order in Perturbative QCD*, Phys. Rev. Lett. **114** (2015) no.14, 142002 [arXiv:1502.01030 [hep-ph]].

[48] T. Becher and M. Neubert, *Infrared singularities of QCD amplitudes with massive partons*, Phys. Rev. D **79** (2009) 125004 [erratum: Phys. Rev. D **80** (2009) 109901] [arXiv:0904.1021 [hep-ph]].

[49] A. Mitov and S. Moch, *The Singular behavior of massive QCD amplitudes*, JHEP **05** (2007) 001 [arXiv:hep-ph/0612149 [hep-ph]].

[50] G.P. Korchemsky and A. V. Radyushkin, *Renormalization of the Wilson Loops Beyond the Leading Order*, Nucl. Phys. B **283** (1987) 342–364.

[51] N. Kidonakis, *Two-loop soft anomalous dimensions and NNLL resummation for heavy quark production*, Phys. Rev. Lett. **102** (2009) 232003 [arXiv:0903.2561 [hep-ph]].

[52] A. Grozin, J.M. Henn, G.P. Korchemsky and P. Marquard, *Three Loop Cusp Anomalous Dimension in QCD*, Phys. Rev. Lett. **114** (2015) no.6, 062006 [arXiv:1409.0023 [hep-ph]].

[53] A. Grozin, J.M. Henn, G.P. Korchemsky and P. Marquard, *The three-loop cusp anomalous dimension in QCD and its supersymmetric extensions*, JHEP **01** (2016) 140 [arXiv:1510.07803 [hep-ph]].

[54] J. Lagrange, Nouvelles recherches sur la nature et la propagation du son, Miscellanea Taurinensis, t. II, 1760-61; Oeuvres t. I, p. 263.

[55] C.F. Gauß, *Theoria attractionis corporum sphaeroidicorum ellipticorum homogeneorum methodo novo tractate*, Commentationes societas scientiarum Gottingensis recentiores, Vol III, 1813, Werke Bd. **V** pp. 5–7.

[56] G. Green, Essay on the Mathematical Theory of Electricity and Magnetism, Nottingham, 1828 [Green Papers, pp. 1–115].

[57] M. Ostrogradsky (presented: November 5, 1828 ; published: 1831) *Première note sur la théorie de la chaleur*, Mémoires de l'Académie impériale des sciences de St. Pétersbourg, series 6, 1: 129–133.

[58] K.G. Chetyrkin and F.V. Tkachov, *Integration by Parts: The Algorithm to Calculate β Functions in 4 Loops*, Nucl. Phys. B **192** (1981) 159–204.

[59] S. Laporta, *High precision calculation of multiloop Feynman integrals by difference equations*, Int. J. Mod. Phys. A **15** (2000) 5087–5159 [hep-ph/0102033].

[60] P. Marquard and D. Seidel, *The* `Crusher` *algorithm*, unpublished.

[61] J. Blümlein and C. Schneider, *The Method of Arbitrarily Large Moments to Calculate Single Scale Processes in Quantum Field Theory*, Phys. Lett. B **771** (2017) 31–36, [arXiv:1701.04614 [hep-ph]].

[62] J. Blümlein, D.J. Broadhurst and J.A.M. Vermaseren, *The Multiple Zeta Value Data Mine*, Comput. Phys. Commun. **181** (2010) 582–625 [arXiv:0907.2557 [math-ph]].

[63] L. Lewin, Dilogarithms and associated functions, (Macdonald, London, 1958).

[64] L. Lewin, Polylogarithms and associated functions, (North Holland, New York, 1981).

[65] A. Devoto and D.W. Duke, *Table of Integrals and Formulae for Feynman Diagram Calculations*, Riv. Nuovo Cim. **7N6** (1984) 1–39.

[66] M. Kauers, *Guessing Handbook*, JKU Linz, Technical Report RISC 09–07.

[67] J. Blümlein, M. Kauers, S. Klein and C. Schneider, *Determining the closed forms of the $O(a_s^3)$ anomalous dimensions and Wilson coefficients from Mellin moments by means of computer algebra*, Comput. Phys. Commun. **180** (2009) 2143–2165 [arXiv:0902.4091 [hep-ph]].

[68] M. Kauers, M. Jaroschek, and F. Johansson, *Ore Polynomials in Sage*, in: Computer Algebra and Polynomials, Editors: J. Gutierrez, J. Schicho, Josef, M. Weimann, Eds.. Lecture Notes in Computer Science **8942** (Springer, Berlin, 2015) 105–125 [arXiv:1306.4263 [cs.SC]].

[69] C. Schneider, *Symbolic Summation Assists Combinatorics*, Sém. Lothar. Combin. **56** (2007) 1–36 article B56b.

[70] C. Schneider, *Simplifying Multiple Sums in Difference Fields*, in: Computer Algebra in Quantum Field Theory: Integration, Summation and Special Functions Texts and Monographs in Symbolic Computation eds. C. Schneider and J. Blümlein (Springer, Wien, 2013) 325–360 [arXiv:1304.4134 [cs.SC]].

[71] C. Schneider, *Modern Summation Methods for Loop Integrals in Quantum Field Theory: The Packages Sigma, EvaluateMultiSums and SumProduction*, J. Phys. Conf. Ser. **523** (2014) 012037 [arXiv:1310.0160 [cs.SC]].

[72] M. Karr, *Summation in finite terms*, J. ACM **28** (1981) 305–350.

[73] C. Schneider, *Symbolic summation in difference fields* Ph.D. Thesis RISC, Johannes Kepler University, Linz technical report 01-17 (2001).

[74] C. Schneider, *A symbolic summation approach to find optimal nested sum representations* in: Motives, Quantum Field Theory, and Pseudodifferential Operators (Clay Mathematics Proceedings Vol. **12**) ed. A. Carey, D. Ellwood, S. Paycha and S. Rosenberg,(Amer. Math. Soc) (2010), 285–308 [arXiv:0904.2323].

[75] C. Schneider, *Fast algorithms for refined parameterized telescoping in difference fields*, in: Computer Algebra and Polynomials, Applications of Algebra and Number Theory, J. Gutierrez, J. Schicho, M. Weimann (ed.), Lecture Notes in Computer Science (LNCS) 8942 (2015), 157–191 [arXiv:13077887 [cs.SC]].

[76] C. Schneider, *A refined difference field theory for symbolic summation*, J. Symbolic Comput. **43** (2008) 611–644 [arXiv:0808.2543].

[77] C. Schneider, *A difference ring theory for symbolic summation*, J. Symb. Comput. **72** (2016) 82–127 [arXiv:1408.2776 [cs.SC]].

[78] C. Schneider, *Summation Theory II: Characterizations of $R\Pi\Sigma^*$-extensions and algorithmic aspects*, J. Symb. Comput. **80** (2017) 616–664 [arXiv:1603.04285 [cs.SC]].

[79] E.D. Ocansey and C. Schneider, *Representation of hypergeometric products of higher nesting depths in difference rings*, J. Symbol. Comput. **120** (2024) 1–50 [arXiv:2011.08775 [cs.SC]].

[80] C. Schneider, *Refined telescoping algorithms in $R\Pi\Sigma$-extensions to reduce the degrees of the denominators* arXiv:2302.03563 [cs.SC].

[81] M. Bronstein, *On solutions of linear ordinary difference equations in their coefficient field*, J. Symbolic Comput. **29** (2000) 841–877.

[82] S.A. Abramov, M. Petkovšek, *D'Alembertian solutions of linear differential and difference equations* in Proc. ISSAC'94, ed. J. von zur Gathen (ACM Press) pp. 169–174.

[83] C. Schneider, *A collection of denominator bounds to solve parameterized linear difference equations in $\Pi\Sigma$-extensions*, An. Univ. Timisoara Ser. Mat.-Inform. **42** (2004) 163–179.

[84] C. Schneider, *Solving parameterized linear difference equations in terms of indefinite nested sums and products*, J. Differ. Equations Appl. **11** (2005) 799–821.

[85] C. Schneider, *Degree bounds to find polynomial solutions of parameterized linear difference equations in $\Pi\Sigma$-Fields*, Appl. Algebra Engrg. Comm. Comput. **16**(2005) 1–32.

[86] C. Schneider, S.A. Abramov, M. Bronstein, M. Petkovšek, C. Schneider, *On rational and hypergeometric solutions of linear ordinary difference equations in* $\Pi\Sigma^*$*-field extensions*, J. Symbolic Comput. **107** (2021) 23–66 [arXiv:2005.04944].

[87] J. Ablinger, *A Computer Algebra Toolbox for Harmonic Sums Related to Particle Physics*, Diploma Thesis, JKU Linz, 2009, arXiv:1011.1176 [math-ph].

[88] J. Ablinger, *Computer Algebra Algorithms for Special Functions in Particle Physics*, Ph.D. Thesis, Linz U. (2012) arXiv:1305.0687 [math-ph].

[89] J. Ablinger, J. Blümlein, C. G. Raab and C. Schneider, *Iterated Binomial Sums and their Associated Iterated Integrals*, J. Math. Phys. **55** (2014) 112301 [arXiv:1407.1822 [hep-th]].

[90] J. Ablinger, A. Behring, J. Blümlein, A. De Freitas, A. von Manteuffel and C. Schneider, *Calculating Three Loop Ladder and V-Topologies for Massive Operator Matrix Elements by Computer Algebra*, Comput. Phys. Commun. **202** (2016) 33–112 [arXiv:1509.08324 [hep-ph]].

[91] T. Gehrmann and E. Remiddi, *Numerical evaluation of harmonic polylogarithms*, Comput. Phys. Commun. **141** (2001) 296–312 [hep-ph/0107173].

[92] J. Ablinger, J. Blümlein, M. Round and C. Schneider, *Numerical Implementation of Harmonic Polylogarithms to Weight* $w = 8$, Comput. Phys. Commun. **240** (2019) 189–201 [arXiv:1809.07084 [hep-ph]].

[93] J. Blümlein, Code `Cpoly.f`, `https://www-zeuthen.desy.de/~blumlein/`

[94] J. Vollinga and S. Weinzierl, *Numerical evaluation of multiple polylogarithms*, Comput. Phys. Commun. **167** (2005) 177–194 [arXiv:hep-ph/0410259 [hep-ph]].

[95] J Blümlein, A. De Freitas, P. Marquard, and C. Schneider. *Challenges for analytic calculations of the massive three-loop form factors.* PoS (LL2024) 031 pages 1–18 [arXiv:2408.07046 [hep-ph]].

[96] S. Gerhold, *Uncoupling systems of linear Ore operator equations*. Master's thesis, RISC, J. Kepler University Linz, 2 2002, Master thesis.

[97] B. Zürcher, *Rationale Normalformen von pseudo-linearen Abbildungen*. Master's thesis, ETH Zürich, 1994.

[98] A. Bostan, Fr. Chyzak, and É. de Panafieu. *Complexity estimates for two uncoupling algorithms*. In Proc. ISSAC'13, Boston, June 2013.

[99] J. Blümlein, P. Marquard and C. Schneider, *A refined machinery to calculate large moments from coupled systems of linear differential equations*, POS (RADCOR2019) 078, pp. 1–15 [arXiv:1912.04390 [cs.SC]].

[100] J. Blümlein, S. Klein, C. Schneider and F. Stan, *A Symbolic Summation Approach to Feynman Integral Calculus*, J. Symb. Comput. **47** (2012) 1267–1289 [arXiv:1011.2656 [cs.SC]].

[101] N. Fadeev, *Computer algebra for special functions*. PhD thesis, RISC, Johannes Kepler University Linz, May 2025.

[102] M. Kauers. D-Finite Functions. (Springer, Cham, CH, 2023).

[103] M. Kauers and P. Paule, The Concrete Tetrahedron. Text and Monographs in Symbolic Computation, (Springer, Wien, 2011).

[104] J. Ablinger, C. Schneider, A. Behring, J. Blümlein and A. de Freitas, *Algorithms to solve coupled systems of differential equations in terms of power series*, PoS (LL2016) 005 [arXiv:1608.05376 [cs.SC]].

[105] J. Blümlein, P. Marquard and C. Schneider, *A refined machinery to calculate large moments from coupled systems of linear differential equations*, PoS (RADCOR2019) 013 [arXiv:1912.04390 [cs.SC]].

[106] J. Ablinger, J. Blümlein and C. Schneider, *Harmonic Sums and Polylogarithms Generated by Cyclotomic Polynomials*, J. Math. Phys. **52** (2011) 102301 [arXiv:1105.6063 [math-ph]].

[107] E. Remiddi and J.A.M. Vermaseren, *Harmonic polylogarithms*, Int. J. Mod. Phys. A **15** (2000) 725–754 [hep-ph/9905237].

[108] J.A.M. Vermaseren, *Harmonic sums, Mellin transforms and integrals*, Int. J. Mod. Phys. A **14** (1999) 2037–2076 [hep-ph/9806280].

[109] J. Blümlein and S. Kurth, *Harmonic sums and Mellin transforms up to two loop order*, Phys. Rev. D **60** (1999) 014018 [hep-ph/9810241].

[110] H. Ferguson and R. Forcade, *Generalization of the Euclidean algorithm for real numbers to all dimensions higher than two*, Bull. Am. Math. Soc. **1** (1979) 912–914.

[111] H. Ferguson and D. Bailey, *A Polynomial Time, Numerically Stable Integer Relation Algorithm*, Technical Report RNR-91-032 (1991).

[112] D.H. Bailey and D.J. Broadhurst, *Parallel integer relation detection: Techniques and applications*, Math. Comput. **70** (2001) 1719–1736 [arXiv:math/9905048 [math.NA]].

[113] S.A. Abramov, D. Khmelnov, A. Ryabenko, *On truncated series involved in exponential-logarithmic solutions of truncated LODEs*, In: Computer Algebra in Scientific Computing, CASC 2022, pp. 18–28, 2022.

[114] M. Mezzarobba, *Rigorous multiple-precision evaluation of D-finite functions in Sagemath*, 5th International Congress on Mathematical Software (ICMS 2016), Berlin, Germany (2016), arXiv:1607.01967v1 [cs.SC].

[115] J. van der Hoeven. *Fast evaluation of holonomic functions near and in singularities*. J. Symbol. Comput. **31** (2001) 717–743.

[116] J. von zur Gathen and J. Gerhard, Modern Computer Algebra. (Cambridge University Press, Cambridge, 2013) 3rd edition.

[117] The FLINT team, `FLINT`*: Fast Library for Number Theory*, 2026. Version 3.4.0, `https://flintlib.org`.

[118] D.J. Broadhurst, *Massive three - loop Feynman diagrams reducible to SC* primitives of algebras of the sixth root of unity*, Eur. Phys. J. C **8** (1999) 311–333 [hep-th/9803091].

[119] A. Hurwitz, *Einige Eigenschaften der Dirichlet'schen Functionen* $F(s) = \sum \left(\frac{D}{n}\right) \cdot \frac{1}{n}$*, die bei der Bestimmung der Classenanzahlen binärer quadratischer Formen auftreten*, Z. Math. Phys. **27** (1882) 86–101; Mathematische Werke, **I** Funktiontheorie 72–88 (Birkhäuser, Basel 1932).

[120] T. Clausen, *Über die Function* $\sin(\varphi) + (1/2^2)\sin(2\varphi) + (1/3^2)\sin(3\varphi)$ *+ etc.*, J. reine und angew. Mathematik (Crelle) **8** (1832) 298–300.

[121] J. Ablinger, J. Blümlein and C. Schneider, *Iterated integrals over letters induced by quadratic forms*, Phys. Rev. D **103** (2021) no.9, 096025 [arXiv:2103.08330 [hep-th]].

[122] J. Blümlein, N. Fadeev and C. Schneider, *Computing Mellin Representations and Asymptotics of Nested Binomial Sums in a Symbolic Way: The RICA Package*, ACM Commun. Comp. Alg. **57** (2023) no.2, 31–34 [arXiv:2308.06042 [hep-ph]].

[123] A.I. Davydychev and M.Y. Kalmykov, *Massive Feynman diagrams and inverse binomial sums*, Nucl. Phys. B **699** (2004) 3–64 [arXiv:hep-th/0303162 [hep-th]].

[124] S. Weinzierl, *Expansion around half integer values, binomial sums and inverse binomial sums*, J. Math. Phys. **45** (2004) 2656–2673 [arXiv:hep-ph/0402131 [hep-ph]].

[125] E.E. Kummer, *Ueber die Transcendenten, welche aus wiederholten Integrationen rationaler Formeln entstehen*, J. Reine Angew. Math. (Crelle) **21** (1840) 74–90.

[126] E.E. Kummer, *Ueber die Transcendenten, welche aus wiederholten Integrationen rationaler Formeln entstehen (Fortsetzung)*, J. Reine Angew. Math. (Crelle) **21** (1840) 193–225.

[127] E.E. Kummer, *Ueber die Transcendenten, welche aus wiederholten Integrationen rationaler Formeln entstehen (Fortsetzung)*, J. Reine Angew. Math. (Crelle) **21** (1840) 328–371.

[128] H. Poincaré, *Sur les groupes des équations linéaires*, Acta Math. **4** (1884) 201–312.

[129] J.A. Lappo-Danilevsky, Mémoirs sur la Théorie des Systèmes Différentielles Linéaires, (Chelsea Publ. Co, New York, 1953).

[130] K.T. Chen, *Algebras of Iterated Path Integrals and Fundamental Groups*, Trans. A.M.S. **156** (3) (1971) 359–379.

[131] A.B. Goncharov, *Multiple polylogarithms, cyclotomy and modular complexes*, Math. Res. Lett. **5** (1998) 497–516 [arXiv:1105.2076 [math.AG]].

[132] S. Moch, P. Uwer and S. Weinzierl, *Nested sums, expansion of transcendental functions and multiscale multiloop integrals*, J. Math. Phys. **43** (2002) 3363–3386 [hep-ph/0110083].

[133] J. Ablinger, J. Blümlein and C. Schneider, *Analytic and Algorithmic Aspects of Generalized Harmonic Sums and Polylogarithms*, J. Math. Phys. **54** (2013) 082301 [arXiv:1302.0378 [math-ph]].

[134] J. Ablinger, *Computing the Inverse Mellin Transform of Holonomic Sequences using Kovacic's Algorithm* PoS (RADCOR2017) 001 [arXiv:1801.01039 [cs.SC]].

[135] https://www.ttp.kit.edu/preprints/2022/ttp22-042

[136] https://gitlab.com/formfactors3l/formfactors3l, https://gitlab.com/formfactors3l/ff3l.